BEST AVAILABLE IMAGES

Defective images within this document are accurate representations of the original documents submitted by the applicant.

Defects in the images may include (but are not limited to):

- BLACK BORDERS
- TEXT CUT OFF AT TOP, BOTTOM OR SIDES
- FADED TEXT
- ILLEGIBLE TEXT
- SKEWED/SLANTED IMAGES
- COLORED PHOTOS
- BLACK OR VERY BLACK AND WHITE DARK PHOTOS
- GRAY SCALE DOCUMENTS

IMAGES ARE BEST AVAILABLE COPY.

As rescanning documents *will not* correct images, please do not report the images to the Image Problem Mailbox.

(12) INTERNATIONAL APPLICATION PUBLISHED UNDER THE PATENT COOPERATION TREATY (PCT)

(19) World Intellectual Property Organization
International Bureau

(43) International Publication Date
6 December 2001 (06.12.2001)

PCT

(10) International Publication Number
WO 01/92078 A2

(51) International Patent Classification[7]: B60T 8/00

(21) International Application Number: PCT/US01/17606

(22) International Filing Date: 31 May 2001 (31.05.2001)

(25) Filing Language: English

(26) Publication Language: English

(30) Priority Data:
09/584,230 31 May 2000 (31.05.2000) US

(71) Applicant *(for all designated States except US)*: **CONTINENTAL AG** [DE/DE]; Vahrenwalder Strasse 9, 30165 Hannover (DE).

(72) Inventor; and

(75) Inventor/Applicant *(for US only)*: **GIUSTINO, James, M.** [US/US]; 8801 Ferngrove Court, Waxhaw, NC 28173 (US).

(74) Agent: **MOORHEAD, Sean, T.**; Calfee, Halter & Griswold LLP, 1400 McDonald Investment Center, 800 Superior Avenue, Cleveland, OH 44114 (US).

(81) Designated States *(national)*: AE, AG, AL, AM, AT, AU, AZ, BA, BB, BG, BR, BY, BZ, CA, CH, CN, CO, CR, CU, CZ, DE, DK, DM, DZ, EC, EE, ES, FI, GB, GD, GE, GH, GM, HR, HU, ID, IL, IN, IS, JP, KE, KG, KP, KR, KZ, LC, LK, LR, LS, LT, LU, LV, MA, MD, MG, MK, MN, MW, MX, MZ, NO, NZ, PL, PT, RO, RU, SD, SE, SG, SI, SK, SL, TJ, TM, TR, TT, TZ, UA, UG, US, UZ, VN, YU, ZA, ZW.

(84) Designated States *(regional)*: ARIPO patent (GH, GM, KE, LS, MW, MZ, SD, SL, SZ, TZ, UG, ZW), Eurasian patent (AM, AZ, BY, KG, KZ, MD, RU, TJ, TM), European patent (AT, BE, CH, CY, DE, DK, ES, FI, FR, GB, GR, IE, IT, LU, MC, NL, PT, SE, TR), OAPI patent (BF, BJ, CF, CG, CI, CM, GA, GN, GW, ML, MR, NE, SN, TD, TG).

Published:
— *without international search report and to be republished upon receipt of that report*

For two-letter codes and other abbreviations, refer to the "Guidance Notes on Codes and Abbreviations" appearing at the beginning of each regular issue of the PCT Gazette.

(54) Title: SYSTEM AND METHOD FOR PREDICTING TIRE FORCES USING TIRE DEFORMATION SENSORS

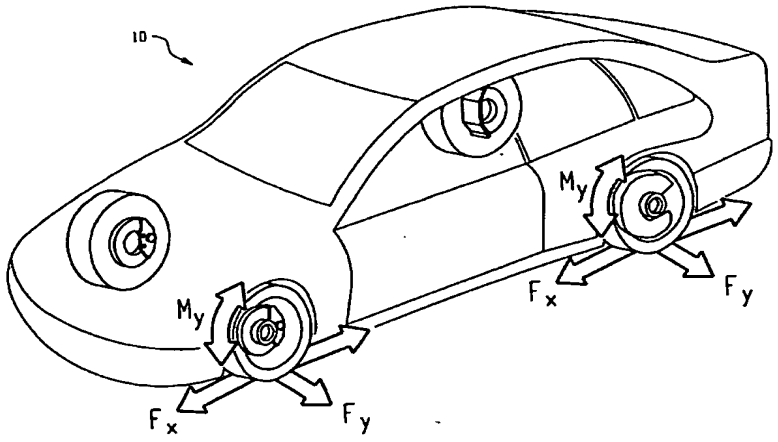

(57) Abstract: A system and method for predicting the forces generated in the tire contact patch from measurements of tire deformations, including separating the lateral force, the vertical force, and the circumferential torque using measurements of tire deformations. A system and method for using a trained neural network or bilinear equations to determine any combination or permutation of one or more of any of the following from tire sidewall deformation sensors, e.g., magnetic tire sidewall torsion measuring (SWT) sensors: the lateral force acting on the tire, the circumferential torque acting on the tire, the longitudinal force acting on the tire, the vertical force acting on the tire, and forces and/or torques having any one or more of the foregoing as components thereof.

WO 01/92078 A2

SYSTEM AND METHOD FOR PREDICTING TIRE FORCES USING TIRE DEFORMATION SENSORS

Field of the Invention

The present invention relates generally to the field of tire dynamics and more specifically to predicting the forces generated in the tire contact patch from measurements of tire deformations, including separating the lateral force and the circumferential torque using measurements of tire deformations.

Background of the Invention

U.S. Pat. No. 5,895,854, which is incorporated herein by reference, discloses a vehicle wheel that is provided with a pneumatic (rubber) tire having at least at one predetermined location a rubber mixture that is permeated with magnetizable particles that have been magnetized. As stated in that patent, the tire disclosed therein can be used in a slip regulation system. Preferably, the magnetized locations are located in one or more annular bands in the sidewall of the tire, i.e., in the longitudinal or peripheral direction, and have successive zones of different magnetization in one or more rows disposed at different radii along the peripheral direction of the tire. It was an object of that patent to provide a vehicle wheel having a pneumatic (rubber) tire, with the aid of which the information required for operating a modern vehicle, e.g. wheel rotational speed for ABS (Anti-lock Brake system) and/or longitudinal forces (torsional forces) that act upon the tire for regulating slipping, can be made available.

According to that patent, the generated magnetization and the spatial magnetization differences could be detected with magnetic field sensors and can serve as SWT sensor input signals (sidewall torsion sensor input signals) for slip regulating systems, especially also for SWT systems (sidewall torsion measuring systems). As further stated in that patent, it was previously thought that in order to be able to detect a change of the time span between the passes of the two marks (in one row for ABS or in two rows for SWT) as precisely as possible, it was desired that the magnetization in the peripheral direction be effected as quadrilaterally as possible, i.e. that the magnetization should be substantially homogeneous within a cohesive region (code bars), and above all at the boundaries of this region should change with as great a gradient as possible. In contrast, it was stated that for the conventional ABS systems that detected the wheel rotations, it was sufficient if the magnetization in the peripheral direction of the tire be effected in a sinusoidal manner.

Thus, a primary function of the SWT system using the SWT sensor has always been to measure the torsional deformation in the tangential direction of the tire and use that torsional deformation to calculate the applied driving or braking torque. However, cornering maneuvers adversely affect the calculation of driving torque or braking torque, because the presence of lateral forces on the tire confounds the measurement of longitudinal torque using the SWT sensor as originally envisioned (using phase differences between the two sensors detecting the magnetic bands in the tire sidewall to calculate torsional deformation). Additionally, the presence of a vertical force on the tire further confounds the measurement of longitudinal torque using the SWT sensor as originally envisioned, although not as severely as lateral force does.

Summary of the Invention

The present invention provides a system and method for not only decoupling the lateral and tangential forces to allow the SWT sensor to be used to effectively measure longitudinal torque, but also predicting the lateral force and other forces and torques acting on the tire using the SWT sensors.

According to the present invention, a system and method are provided for predicting the forces generated in the tire contact patch from measurements of tire deformations, including separating skewed forces, e.g., lateral force and circumferential torque, using measurements of tire deformations.

According to one aspect of the system of the present invention, a trained processor, e.g., a trained neural network, is used to predict skewed forces, e.g., lateral force and circumferential torque, using measurements of tire deformations. In a first embodiment, a trained neural network is used to predict at least one force acting on the tire, preferably lateral force and circumferential torque. In a second embodiment, a set of bilinear equations are used to predict at least one force acting on the tire, preferably lateral force and circumferential torque.

It is therefore an advantage of the present invention to provide a system and method for determining circumferential torque using tire deformation sensors, e.g., SWT sensors.

It is also an advantage of the present invention to provide a system and method for determining lateral force using tire deformation sensors, e.g., SWT sensors.

It is therefore another advantage of the present invention to provide a system and method for decoupling lateral force and circumferential torque in measurements from tire deformation sensors, e.g., SWT sensors.

It is a further advantage of this invention to provide a system and method for determining vehicle yaw rate from tire deformation sensors, e.g., SWT sensors, thereby eliminating the need for a separate yaw rate sensor.

It is yet another advantage of the present invention to provide a system and method for determining vehicle speed from tire deformation sensors, e.g., SWT sensors, thereby eliminating the need for a separate speed sensor.

It is still another advantage of the present invention to provide a system and method for using a trained neural network to determine any combination or permutation of one or more of any of the following from tire deformation sensors, e.g., SWT sensors: the lateral force acting on the tire, the circumferential torque acting on the tire, the longitudinal force acting on the tire, the vertical force acting on the tire, and forces and/or torques having any one or more of the foregoing as components thereof.

It is further still another advantage of the present invention to provide a system and method for using bilinear equations to determine any combination or permutation of one or more of any of the following from tire deformation sensors, e.g., SWT sensors: the lateral force acting on the tire, the circumferential torque acting on the tire, the longitudinal force acting on the tire, the vertical force acting on the tire, and forces and/or torques having any one or more of the foregoing as components thereof.

It is another advantage of the present invention to decouple circumferential torque of a tire from lateral forces and vertical forces acting on the tire.

It is still another advantage of the present invention to provide a system and method for determining any combination or permutation of one or more of any of the following from tire sidewall deformation sensors, e.g., SWT sensors: the lateral force acting on the tire, the circumferential torque acting on the tire, the longitudinal force acting on the tire, the vertical force acting on the tire, and forces and/or torques having any one or more of the foregoing as components thereof.

These and other advantages of the present invention will become more apparent from a detailed description of the invention.

Brief Description of the Drawings

In the accompanying drawings, which are incorporated in and constitute a part of this specification, embodiments of the invention are illustrated, which, together with a general

description of the invention given above, and the detailed description given below serve to example the principles of this invention.

Figure 1 is a perspective view of a vehicle showing various forces and torques;

Figure 2 is a schematic block diagram of a system of the present invention;

Figure 3 is a side view of a tire having magnetic bands of alternating polarity and corresponding sensors used with the system and method of the present invention;

Figure 4 is a perspective view of a mounting bracket fixed to a suspension strut and holding two magnetic sensors in close proximity to the magnetic sidewall of the tire;

Figure 5 is a close up view of the mounting bracket and sensors shown in Figure 5;

Figure 6 is a front view of the tire, suspension strut, and sensors showing the effects of a lateral force, with the tire viewed in a section taken vertically;

Figure 7 is a close up view of the tire and sensors of Figure 6;

Figure 8 is a data plot of SWT sensor amplitude taken in the presence of lateral force and circumferential torque, showing that in the presence of torque SWT sensor amplitude is a relatively poor predictor of lateral force;

Figure 9 is a data plot of SWT sensor amplitude taken in the presence of lateral force and circumferential torque, showing that the presence of lateral force causes a cross-term error when using SWT sensor phase difference as a predictor of circumferential torque;

Figure 10 is a flow chart showing the general procedure used to train the neural network of the present invention;

Figure 11 is a flow chart showing the general procedure for using the trained neural network of the present invention to predict lateral force and circumferential torque;

Figure 12 is a data plot showing the lateral force and circumferential torque applied to the tire during data acquisition;

Figure 13 is a schematic block diagram showing the structure of the neural network trained in Example 1;

Figure 14 is a data plot showing measured lateral force and the lateral force predicted by the trained neural network of Example 1;

Figure 15 is a data plot showing measured circumferential torque and the circumferential torque predicted by the trained neural network of Example 1;

Figure 16 is a data plot showing measured lateral force and the lateral force predicted by the bilinear equations of Example 2;

Figure 17 is a data plot showing measured circumferential torque and the circumferential torque predicted by the bilinear equations of Example 2;

Figure 18 is a data plot showing measured vertical force and the vertical force predicted by the trained neural network of Example 3;

Figure 19 is a data plot showing measured lateral force and the lateral force predicted by the trained neural network of Example 3;

Figure 20 is a data plot showing measured circumferential torque and the circumferential torque predicted by the trained neural network of Example 3;

Figure 21 shows a plurality of coefficient of dynamic friction (μ) versus percent slip (μ-slip) curves at various steering angles showing the significant effect that even small lateral forces can have on the location of the peak of the μ-slip curve;

Figure 22 is a data plot showing measured vertical force and the vertical force predicted by the bilinear equations of Example 4;

Figure 23 is a data plot showing measured lateral force and the lateral force predicted by the bilinear equations of Example 4; and

Figure 24 is a data plot showing measured circumferential torque and the circumferential torque predicted by the bilinear equations of Example 4.

Detailed Description of the Preferred Embodiment

"Circuit communication" as used herein is used to indicate a communicative relationship between devices. Direct electrical and optical connections and indirect electrical and optical connections are examples of circuit communication. Two devices are in circuit communication if a signal from one is received by the other, regardless of whether the signal is modified by some other device. For example, two devices separated by one or more of the following—transformers, optoisolators, digital or analog buffers, analog integrators, other electronic circuitry, fiber optic transceivers, or even satellites—are in circuit communication if a signal from one reaches the other, even though the signal is modified by the intermediate device(s). As a final example, two devices not directly connected to each other, but both capable of interfacing with a third device, e.g., a CPU, are in circuit communication. As used herein, "input" refers to either a signal or a value and "output" refers to either a signal or a value.

Referring now to Fig. 1, the forces referred to herein are shown schematically. In that figure, a vehicle 10 is shown schematically along with the longitudinal force F_x, the

longitudinal (circumferential) torque M_y, and the lateral force F_y acting on the tires. Although not shown in Figure 1, another force of interest is the vertical force F_z which is perpendicular to the longitudinal force F_x and the lateral force F_y.

Referring now to Fig. 2, a vehicle control system 20 according to the present invention is shown schematically. In the broadest sense, the vehicle control system 20 comprises a force prediction unit 22 to be placed in circuit communication with at least one tire sidewall deformation sensor. Preferably, the tire sidewall deformation sensor is a magnetic tire sidewall torsion (SWT) sensor. The force prediction unit 22 has a preprogrammed processor (not shown) that receives input from the at least one SWT sensor and at least one other sensor input and performs data analysis by implementing preprogrammed equations having constants determined from previously collected data to determine from at least the SWT input and the at least one other sensor input an output corresponding to a predicted circumferential torque and/or longitudinal force and/or lateral force and/or vertical force acting on the tire. The force prediction unit 22 may also perform any necessary signal conditioning and data processing associated with the SWT sensor and the other sensor.

With respect to Fig. 2, in a preferred embodiment, the force prediction unit 22 is placed in circuit communication with a pair of magnetic SWT sensors 26, 28 for each tire 30 of the vehicle 20; however, the force prediction unit 22 may be used with as little as one SWT sensor 26 on a single tire 30 and another sensor, e.g., another SWT sensor 28 or an ABS speed sensor (not shown) to provide force predictions about that one tire 30. Preferably, the force prediction unit 22 is placed in circuit communication with a control unit 32, which is in circuit communication with and affects the dynamic state of the vehicle 20 via one or more actuators 34. Examples of control units 32 and actuators 34 known to those in the art include combinations and permutations of one or more of the following: an ABS control unit with braking actuators, a traction control system (TCS) control unit with braking and throttle actuators, an electronic stability control (ESC) (also known as an integrated vehicle dynamics (IVD)) control unit with braking and throttle actuators, a locked differential control unit, a suspension control unit, a brake assist control unit with braking actuators, an intelligent cruise control unit with vehicle throttle actuators, a steering assist control unit with steering actuators, a deflation detection control unit, a navigation control unit, a rollover prevention control unit, and a brake-by-wire control unit with braking actuators. Significantly, these exemplary control units 32 and actuators 34 require one of more of the following sensors--a longitudinal accelerometer (for longitudinal force and/or acceleration), a lateral accelerometer

(for lateral force and/or acceleration), a vertical load sensor, wheel speed sensors, and a yaw rate sensor, all of which can be replaced by one or more SWT sensors coupled with the teachings of the present invention.

The force prediction unit 22 can be implemented with various combinations of analog and digital circuitry, processors, and the like. The control unit can be implemented with separate circuitry and/or processor(s) or with circuitry and/or processor(s) used to implement the force prediction unit 22. Preferably, the data processing and data analysis portions of the force prediction unit 22 are implemented in a single processor, with the signal conditioning being performed in dedicated analog circuitry (not shown).

Referring now to Fig. 3, a pair of SWT sensors 26, 28 is shown schematically with the corresponding magnetic tire 30. As shown schematically in Fig. 3, the magnetic tire 30 used with the SWT sensors 26, 28 preferably has a number of alternating bands 38 of magnetic polarity. The magnetic tires 30 can be made in any number of ways, e.g., as taught in U.S. Pat. No. 5,895,854, as taught in copending U.S. Patent Application No. 09/347,757, which is incorporated herein by reference, or in any number of other ways, e.g., providing alternating bands of premagnetized thin material, embedding adjacent alternating magnetic bands into the sidewall of a green tire, and curing the green tire. The SWT sensors 26, 28 themselves are preferably magnetic sensors, e.g., magneto-resistive (MR) sensors, Hall effect sensors, or flux gate sensors, positioned close enough to the magnetic regions of the sidewall of tire 30 to interact therewith. MR sensors have the advantages of allowing a moderate air gap and have been extensively tested. Flux gate sensors have the advantage of allowing an air gap of between one to two inches. Hall effect sensors have the disadvantage of requiring a relatively small air gap. If two SWT sensors are used, one sensor 26 is preferably positioned near the tread 40 and the other sensor 28 is preferably positioned near the bead 42. If only one SWT sensor is used with another sensor, e.g., an ABS speed sensor, the SWT sensor 26 is preferably positioned closer to the tread 40 than the bead 42 to provide greater sensitivity to torsional deformation.

Referring now to Fig. 4 and Fig. 5, the mounting of the sensors 26, 28 to a vehicle suspension strut 50 is shown. Preferably the sensors 26, 28 are mounted to a suspension strut 50 via a mounting bracket 52. In Fig. 4 and Fig. 5, the sensors 26, 28 are model number KMZ10A magneto-resistive (MR) sensors, available from Philips. Mounting bracket 52 preferably is configured so that the flat end portion of hall effect sensors 26, 28 are substantially parallel to the sidewall of magnetic tire 30. Preferably, the flat end portion of

MR sensors 26, 28 are 12.5 mm from the surface of the sidewall of magnetic tire 30 when there are no lateral forces present acting on the tire 30. With lateral forces present, the air gap can be expected to range from about 8 mm to about 25 mm. Because the sidewall of a tire typically has a pronounced curvature, the mounting bracket 52 preferably provides a pair of skewed (i.e., not parallel) surfaces 54, 56 for the sensors 26, 28 respectively. The mounting bracket 52 may be secured to suspension strut 50 by any suitable means, such as integrally forming mounting bracket 52 with strut 50, using suitable fasteners, e.g., bolts 58 and nuts 60 as shown in Figs. 4 and 5, or by any other suitable means. The sensors 26, 28 may be secured to mounting bracket 52 by any suitable means, such as using suitable fasteners, e.g., bolts 62 and nuts 64 as shown in Figs. 4 and 5, or by any other suitable means. Wires 66, 68 place sensors 26, 28 in circuit communication with the force prediction unit 22.

The mounting bracket also preferably secures sensors 26, 28 so that the line segment between them is as parallel as is practicable to the magnetic interface line between successive magnetic bands 38 of magnetic tire 30. In this way, in the free rolling state, the sensors 26, 28 preferably detect the transition from one band 38 to the next at the same time, i.e., there will be no or a small phase difference between the two sensor signals. A torsional deformation, e.g., caused by application of a brake, takes the form of the tire tread 40 rotating with respect to the tire bead 42, so that the tire magnetic interface line is no longer parallel to the line segment between sensors 26, 28. This torsional deformation is detected by the SWT sensors 26, 28 as a change in the phase shift between the two signals, i.e., the transition from one magnetic band 38 to the next will be detected by one sensor sooner or later than it would otherwise be detected by that sensor with respect to the other sensor. The signals from the sensors 26, 28 in this configuration are sinusoidal signals.

The sensors 26, 28 in Figure 4 and Figure 5 are positioned at the 180° location (at the 12 o'clock position), which provides the most sensitivity for decoupling circumferential torque and lateral force, F_y. Additionally, it is preferable to position a second pair of SWT sensors per tire (not shown) at either the 90° or the 270° position (at the 3 o'clock or 9 o'clock position) to provide the most sensitivity for decoupling circumferential torque and vertical force, F_z. However, providing sensors at the 90° or the 270° position has proven to be challenging because sensors in either of those positions tend to be exposed to forces that misalign the sensors or cause the sensor supports to bend or break off. In the alternative, a single pair of SWT sensors positioned at 135° is believed to provide information to decouple circumferential torque from both lateral force, F_y, and vertical force, F_z. Also in the

alternative, a single additional outer sensor can be used at either the 90° or the 270° position rather than using an additional pair of sensors in that position. In that case, the phase of the sensor at the 90° or 270° position would be taken with respect to the inner sensor at the 180° position.

The force prediction unit 22 preferably accepts as inputs at least (a) a phase difference input, relating to (and preferably representing) a change in phase between the signals of the two sensors 26, 28 caused by torsional deformation in the sidewall of the tire and (b) a peak amplitude input from the outer sensor 26 relating to (and preferably representing) the length of the changing air gap between the sensor 26 and the sidewall. More preferably, the force prediction unit 22 also accepts as additional inputs (c) a value relating to (and preferably representing) the speed of the vehicle (which can be determined from the period of each region of one of the SWT sensors, inverted and scaled by the radius of the tire) and (d) a delta input relating to (and preferably representing) the difference between the peak amplitude signal from the outer sensor 26 and the peak amplitude signal of the inner sensor 28. The speed input allows the force prediction unit to take into account the effects on the sidewall of centrifugal forces at higher speeds and the effects of relaxation phenomenon on the tire the at lower speeds. Additionally, certain cross terms such as phase difference input multiplied by peak amplitude input allow force prediction units to be trained with a very low mean sum of squared errors. Thus, force prediction units according to the present invention, such as neural networks and bilinear equation sets, can have as inputs any one or more of the following: one phase difference input for each sensor pair, a peak amplitude input for each sensor, preferably each outer sensor in the pair, a speed input, a delta peak input for each sensor pair, and a cross term (phase difference input multiplied by peak amplitude input) for each sensor pair, among others, with sensor pairs being located at 90° and/or 135° and/or 180° and/or 270°, depending on the force(s) and/or torque(s) to me predicted.

Referring now to Fig. 6 and Fig. 7, the effect on the positional relationship between the tire 30 and sensors 26, 28 by a lateral force is shown schematically. The tire 30 and rim 70 are shown in dashed lines in the free rolling state and in solid lines under the influence of a lateral force. In short, the lateral force causes the distance between the sensors 26, 28 and the tire 30 to be greater. A lateral force in the opposite direction to the force shown in Fig. 6 will cause the distance between the sensors 26, 28 and the tire 30 to be less. These

differences in distance are reflected in a change in amplitude of the signals from sensors 26, 28.

The relatively straightforward conceptual framework for the SWT sensors set forth in the preceding two paragraphs is greatly complicated in application because the lateral force and longitudinal force are coupled to some degree. This is illustrated by Fig. 8 and Fig. 9. Fig. 8 shows plots of normalized lateral force (in the presence of circumferential torque) and normalized amplitude of the outer SWT sensor 26 versus time (data from a Conti Sport Contact, 245/40 R18 magnetic sidewall tire collected with an MTS Model 860 tread wear machine (available from MTS Systems Corporation) in accordance with the data collection section of Example 1). As shown in Fig. 8, in the presence of circumferential torque, the normalized amplitude of the outer SWT sensor 26 is a poor predictor of lateral force. Similarly, Fig. 9 shows plots of normalized circumferential torque (in the presence of lateral force) and normalized phase-shift between the two SWT sensors 26, 28 versus time (data from a Conti Sport Contact, 245/40 R18 magnetic sidewall tire collected with an MTS Model 860 tread wear machine in accordance with the data collection section of Example 1). As shown in Fig. 9, the presence of lateral force apparently causes a cross-term error when using the normalized phase difference between the two SWT sensors 26, 28 as a predictor of circumferential torque.

The present invention overcomes these drawbacks by using the force prediction unit 22 of the present invention, which uses inputs from both SWT sensors 26, 28 to determine both the circumferential torque and the lateral force acting on the tire.

In a first embodiment of the force prediction unit 22 of the present invention, the processor of the force prediction unit 22 implements a neural network either in software or in hardware. Preferably the neural network is configured to determine both the circumferential torque and the lateral force acting on the tire; however, the neural network can be configured to determine any combination or permutation of one or more of any of the following: the lateral force acting on the tire, the circumferential torque acting on the tire, the longitudinal force acting on the tire, the vertical force acting on the tire, and forces and/or torques having any one or more of the foregoing as components thereof. Preferably, the magnitude (amplitude) of the outer SWT sensor 26 and the phase difference between the signals of the two SWT sensors 26, 28 are input to the neural network, with the desired parameters being output. Even more preferably, the difference in magnitude (amplitude) between the signal from the outer SWT sensor 26 and the signal from the inner SWT sensor 28 is used as an

additional input. The neural network of the force prediction unit 22 is preferably a multi-layer perceptron, and is even more preferably a multi-layer perceptron having one input layer, one hidden layer (having, e.g., 5-20 nodes), and one output layer. As to transfer functions between layers, a nonlinear, hyperbolic tangent sigmoidal transfer function is preferably used between the input layer and the hidden layer, and a linear transfer function is preferably used between the hidden layer and the output layer. The hyperbolic tangent sigmoidal transfer function is preferably implemented as follows:

$$\text{tansig} = \frac{2}{e^{-2n} - 1} - 1$$

where

$n = W \cdot p + b$
W = a matrix of weights,
b = a matrix of bias values
p = a matrix of input values
$W \cdot p$ represents matrix multiplication

As expected, the neural network in the force prediction unit 22 must be trained using previously collected data. This training is exemplified by Fig. 10, which is a flowchart 100 showing generally how the neural network in the force prediction unit 22 is trained using previously collected data. Initially, data must be collected, at step 102. In general, the desired forces and torques are collected, e.g., from an instrumented hub or from a dynamometer, along with the raw SWT sensor data. In the preferred embodiment, the circumferential torque and the lateral force acting on the tire, and the raw SWT sensor data, are collected with an MTS Model 860 tread wear machine (available from MTS Systems Corporation) with the frequency of the circumferential torque and lateral force being different prime numbers to provide a full spectrum of measured and interacting torques and forces. Data is collected, for example, at between 25,000 and 1,000,000 samples per second, and typically at 50,000 samples per second.

Next, at step 104, the raw sinusoidal SWT sensor data is processed to calculate the inputs to the neural network. In the preferred embodiment, the phase and two amplitudes are calculated from the peaks and zero-crossings of the raw SWT sensor data. More specifically,

(a) the phase difference is determined as follows: (i) the mean value is subtracted from all the data, (ii) at each peak region and at each valley region a polynomial is fit along the peak or valley, (iii) the maximum/minimum of the resulting polynomial is determined (by, e.g., setting the differential to zero to determine the horizontal tangent), (iv) the time of a peak/valley of one signal is

subtracted from the time of the peak/valley of the other signal, and (v) the resulting difference is divided by the corresponding "half-period" (the time from the previous peak/valley to that valley/peak) to make the phase difference independent of vehicle velocity;

(b) the amplitude of the signal from the outer SWT sensor 26 is determined as follows: (i) the mean value is subtracted from all data from sensor 26, (ii) at each peak region and at each valley region a polynomial is fit along the peak or valley, (iii) the maximum/minimum of the resulting polynomial is determined (by, e.g., setting the differential to zero to determine the horizontal tangent), (iv) the processed signal is rectified (by, e.g., taking the absolute value of each data point), and (v) the amplitude of the fit polynomial at each maximum is used as the amplitude of that signal;

(c) the peak difference between the two SWT signal amplitudes is determined as follows: (a) the peak amplitude of the signal from the inner sensor 28 is calculated in accordance with step (b) above is subtracted from the peak amplitude of the signal from the outer sensor 26 as determined at (b) above.

The sinusoidal nature of the signals from the sensors facilitates using the fit polynomial in place of the actual sensor data. Additionally, using the fit polynomial for the phase and amplitude inputs tends to smooth or remove any noise that might otherwise cause erroneous calculations.

Having calculated the phase and two amplitudes, next these inputs are corrected at step 106 using various correction methods. An exemplary correction method is as follows: For a tire magnetized so that there are 48 north and 48 south poles per circumference, the inner and outer SWT sensor signals will be very much like sinusoidal waves with a frequency of 48 wavelengths per tire revolution; i.e., there are 48 "peak" amplitudes and 48 "valley" amplitudes in every tire revolution. If the mean is subtracted from the signal, each revolution would produce 96 "zero" crossings. In addition, if the signal is rectified, turning each valley into a peak, there would be 96 peak amplitudes. NumPoles represents the number of North and South magnetic poles around the circumference of the tire. Thus, for this particular tire the parameter NumPoles is 96. For a uniform velocity, i.e., for a constant speed with no torques or lateral forces acting, the time difference between the zero crossings, or the time difference between the peak amplitudes, defines the pole pitch. If the pole spacing is uniform, there would be 360 degrees / 96 = 3.75 degrees or 2 Pi / 96 = 0.0654 radians

between each pole. In practice, however, the pole spacing is rarely perfectly uniform for a particular tire. Thus, there is some error associated with each of the 96 pole spacing values. But this error is due to the geometry and magnetization process applied to the particular tire. The error for each pole spacing value repeats itself with each revolution of the tire. These errors affect not only the pole pitch values, but also the phase differences between the inner and outer SWT sensor signals. With no torques or lateral forces acting on the tire, the phase differences between these two signals will consist of 96 constant values. Thus, the following method can be used to correct the phase errors between poles:

First, (1) SWT phase data is collected at a uniform velocity (no torques or lateral forces). Then, (2) from the vector of phase data collected in (1), calculate the zero crossings (or "mean" crossings) and the peaks and valley amplitudes. Next, (3) rectify the data so that valley amplitudes become peak amplitudes. Then, (4) partition the vectored data into NumPoles sets and ensemble average N of the sets, i.e.:

pole number	1	2	3	...	k	...	NumPoles
set 1	p_{11}	p_{12}	p_{13}	...	p_{1k}	...	$p_{1NumPoles}$
set 2	p_{21}	p_{22}	p_{23}	...	p_{2k}	...	$p_{2NumPoles}$
...	...	...	...	...	...	...	...
set j	p_{j1}	p_{j2}	p_{j3}	...	p_{jk}	...	$p_{jNumPoles}$
set N	p_{N1}	p_{N2}	pN3	...	p_{Nk}	...	$p_{NNumPoles}$
Average	ave_1	ave_2	ave_3	...	ave_k	...	$ave_{NumPoles}$

Next, (5) calculate the average (grand mean) of the ensemble averages. Then, (6) subtract the grand mean from the Average vector to form a vector of correction values. Next, (7) subtract the correction values from entire matrix of data collected under the influence of various torques and forces, i.e., correct all the data that has been previously collected. Finally, (8) reshape matrix of data back into a vector.

In the alternative, (9) the data can be filtered data using a running average where the number of points averaged is between 2 and NumPoles.

The amplitude data is corrected in a similar fashion using a multiplicative error correction routine. Perform the same steps 1 through 5 as described in the additive correction error algorithm described above, but apply the steps to the vector of SWT amplitude data. In step 6 however, instead of subtracting the grand mean from the Average, divide the grand

mean into the Average to form the vector of correction values. In step 7, multiply the entire matrix of data by the vector of correction values, thereby correcting all the amplitude data. Steps 8 and 9 are performed the same as for the additive correction value.

Next, at step 108, the corrected phase data and two corrected amplitudes are normalized, i.e., scaled to between -1 and +1 by ordinary techniques known to those in the art.

Then the large data set is divided into various sets, e.g., a training set, a validation set, and a test set, at step 110.

Next, the training data set is used to train the neural network, at step 112. Preferably the neural network is trained using the known Levenberg-Marquardt technique with early stopping. Ordinary back-propagation could be used to train the network, but might take a prohibitively long period of time to converge. Preferably the validation data set is used to determine validation error (mean sum of squared errors), which is used to determine when to stop training the neural network so that the neural network properly generalizes and does not fit noise. More preferably, the neural network is trained until the validation error increases for a specific number of iterations, preferably 5 iterations. The weights from the training iteration immediately before the validation error began increasing (6 iterations back) are used as the final weights. In the alternative, the neural network is trained until the mean sum of squared errors for the training data set is equal to or less than 0.0001.

Finally, the weights are tested using the test data set, at task 116, by applying the test data set to the trained neural network and calculating the mean sum of squared errors. If the mean sum of squared errors is relatively low, preferably on the order of about 0.0018, more preferably lower than 0.0018, then the weights have passed this last test. If the mean sum of squared errors is relatively high, i.e., significantly higher than 0.0018, then an alternative neural network structure should be used, e.g., more or fewer hidden neurons, perhaps an additional hidden layer, etc.

Additionally, the neural network weights can be verified and tested using SWT raw data and force and torque data collected from a vehicle having at least one instrumented hub, e.g., Model 242 electronics and Model 6613 wheel sensor, both from GSE, Inc.

It is currently believed that because each type of tire (e.g., a Conti Sport Contact, P245/40 R18 as compared to an Ameri★G4S P205/70 R15 as compared to an Contitrac AW P275/65 R17) has different static and dynamic characteristics, each type of tire will require separate data collection and training. Additionally, specific variations in specific tires of the

same type might have different enough characteristics to warrant individualized parameters being used by the force prediction unit 22. Accordingly, the processor in the force prediction unit 22 will need to have some means for using the proper neural network weights with the particular type of magnetic tire 30 on the vehicle 10 or specific tire on the vehicle 10. For example, the force prediction unit 22 might have a plurality of pre-loaded weights, number of layers, number of hidden nodes, etc. for a plurality of different types of tires, in which case the force prediction unit 22 need only be apprised of the particular type of tire 30 mounted on the vehicle 10. The force prediction unit 22 can be apprised of the particular type of tire 30 mounted on the vehicle 10 by a number of means, e.g., having one of the SWT sensors read a magnetic code (e.g., a preselected series of magnetic transitions in the form of a bar code or the like embedded into the tire sidewall) directly from the tire sidewall, communicating with an external device 120 (Fig. 2) such as a selectably connectable computer or interface pendant through which the tire type is selected, etc. so that the force prediction unit 22 can associate the proper weights, number of layers, number of hidden nodes, etc. with the tire mounted on the vehicle. In addition, or in the alternative, the force prediction unit 22 can have communication circuitry to directly or indirectly receive neural network parameters such as weights, number of layers, number of hidden nodes, etc. from an external device 120 (Fig. 2) such as a selectably connectable computer or an interface pendant.

In addition, the neural network is preferably dynamically trained to optimize its weights in real-time. To optimize in real time, the presence of valid training data must be determined. Valid SWT sensor data could be determined using various sensors on the vehicle. For example, ESP systems typically have lateral force accelerometers, which could be used to measure lateral force data correlated with collected SWT sensor data. Additionally, engine torque sensors and other sensors could be used to measure circumferential torque correlated with collected SWT sensor data. Such validated data could be used to retrain the neural network to optimize or otherwise alter the neural network weights.

Referring now to Fig. 11, and also back to Fig. 2, once the neural network is trained and the force prediction unit 22 has loaded and/or associated the weights, number of layers, number of hidden nodes, etc. with the mounted tire 30, the force prediction unit 22 predicts forces acting on the tire 30 as generally set forth in routine 200.

After system initialization, as known to those in the art, data must be collected, at step 202. The raw SWT sensor data is collected in a real-time manner. The raw sensor data

is collected, for example, at a rate of at least 100,000 samples per second and input to the processor (e.g., a DSP) in the force prediction unit 22. In the alternative, and preferably, the raw sensor data is collected by analog circuitry that determines mean-crossings (for phase) and peak amplitudes, which are sent to the processor (e.g., a DSP) in the force prediction unit, e.g., by a CAN protocol communications link to be input into the neural network.

Next, at step 204, the raw SWT sensor data is processed to calculate the inputs to the neural network. In the preferred embodiment, the phase and two amplitudes are calculated from the peaks and zero-crossings of the raw SWT sensor data using analog circuitry. For example, the analog circuitry can determine the phase difference with a phase-locked loop (PLL). The analog circuitry can determine the amplitude of the signal from both SWT sensors 26, 28 by integrating each signal, holding at peak values, and returning the peak values. These phase and both peaks are sent to the processor in the force prediction unit, e.g., by a CAN protocol communications link. The processor determines the difference between the two SWT signal amplitudes by subtracting one peak from the other.

Having calculated the phase and two amplitudes, next these inputs are corrected at step 206 using various correction methods. Preferably, the phase data is corrected using the additive correction algorithm discussed above. Preferably, both amplitudes are corrected using the multiplicative error correction algorithm discussed above.

Next, at step 208, the phase data and two amplitudes are normalized, i.e., scaled to between -1 and +1 by ordinary techniques known to those in the art, using the same normalization parameters used to normalize the data at step 108 of Fig. 10.

Finally, the force prediction unit 22 determines the predicted forces using the scaled, corrected data. In general, the force prediction unit 22 determines any combination or permutation of one or more of any of the following: the lateral force acting on the tire, the circumferential torque acting on the tire, the longitudinal force acting on the tire, the vertical force acting on the tire, and forces and/or torques having any one or more of the foregoing as components thereof. These determined forces and torques are referred to herein as "predicted." Preferably, the force prediction unit 22 determines the predicted circumferential torque on the tire. Preferably, the force prediction unit 22 determines the predicted lateral force acting on the tire. Even more preferably, the force prediction unit 22 determines the predicted lateral force acting on the tire and the predicted circumferential torque acting on the tire.

Finally, at task 212, the control unit 32 alters the dynamic state of the vehicle 20 via actuators 34 responsive to the force(s) and/or torque(s) predicted by the force prediction unit 22. In addition, or in the alternative, the control unit can produce a qualitative or quantitative display of any desired parameter on a display unit (not shown). Qualitative displays can be made by comparing predicted forces and/or torques to baseline or threshold forces and/or torques and displaying an appropriate display based on the results of the comparison. Quantitative displays can be numeric displays of predicted force(s) and/or torque(s), and/or values derived therefrom.

In a second embodiment of the force prediction unit 22 of the present invention, the processor of the force prediction unit 22 implements a bilinear equation in software or in hardware. Preferably there are two bilinear equations--one for lateral force and one for circumferential torque. However, the force prediction unit 22 can be configured to determine any combination or permutation of one or more of any of the following using one bilinear equation for each predicted force or torque: the lateral force acting on the tire, the circumferential torque acting on the tire, the longitudinal force acting on the tire, the vertical force acting on the tire, and forces and/or torques having any one or more of the foregoing as components thereof. Preferably, the magnitude (amplitude) of the outer SWT sensor 26 and the phase difference between the signals of the two SWT sensors 26, 28 are used in each bilinear equation. Even more preferably, the difference in magnitude (amplitude) between the signal from the outer SWT sensor 26 and the signal from the inner SWT sensor 28 is used as an additional variable in each bilinear equation. Thus, the bilinear equations are preferably of the form:

$$M_y = k_1 + k_2 \cdot p + k_3 \cdot a + k_4 \cdot d + k_5 \cdot p \cdot a$$

$$F_y = k_6 + k_7 \cdot p + k_8 \cdot a + k_9 \cdot d + k_{10} \cdot p \cdot a$$

Where,

p = SWT Phase at 180 degree position, in radians

a = SWT Amplitude of outer sensor 26 at 180 degree position, in mm

d = Difference between SWT outer and inner amplitudes, in mm

M_y = Circumferential torque, kN-m

F_y = Lateral force, kN

k_1-k_{10} = constants from bilinear fit

The constants k_1-k_{10} are determined using standard multiple linear regression techniques, which are known to those in the art. More specifically, the bilinear equations are

determined as follows. First, steps 102 through 108 are performed as discussed in the text accompanying steps 102-108, resulting in a set of corrected, normalized data. Then the constants k_1-k_{10} are calculated in MATLAB by regressing Y on X as follows:

```
X = [ ones(n,1)  X];
XTXI = inv(X' * X);
COEF = XTXI * X' * Y;
```

where:
n is the number of samples
X is a matrix containing all the phase data, amplitude data, delta data, and phase * amplitude data
Y is the vector of predicted forces/torques

Using the bilinear equation embodiment of the force prediction unit of the present invention is identical to the flowchart of Fig. 11, except at step 210, the force(s) and/or torque(s) are predicted using the bilinear equations rather than using a neural network.

Although the bilinear equations do not appear to perform as well as the trained neural network (see examples below), the predictions from the bilinear equations might well suffice under certain circumstances.

In addition to the forces and torques described above, the present invention can be applied to derive or determine various calculated values that are useful for vehicle control systems. For example, coefficients of friction can be calculated from F_x, F_x, and F_z determined by the present invention (e.g., by using F_z/F_y and F_z/F_x). As another example, yaw rate for the vehicle can be determined by solving the appropriate vehicle dynamics equations that involve integrating the predicted force equations to calculate the appropriate angular rate or angular velocity associated with the yaw moments, determined by the present invention.

Example 1 - Neural Network

First, a Conti Sport Contact, 245/40 R18 magnetic sidewall tire was prepared as generally described in U.S. Pat. No. 5,895,854 and copending U.S. Patent Application No. 09/347,757, with 200 phr (parts per hundred) of strontium ferrite powder embedded in the sidewall prior to curing. The embedded strontium ferrite was magnetized to magnetic saturation using 96 electromagnets providing 48 North poles alternating with 48 South poles.

Next, the Conti Sport Contact tire was mounted on an MTS Model 860 tread wear machine (available from MTS Systems Corporation) as follows: The magnetic sidewall tire

was mounted to a precision rim. Two pairs of SWT sensors (Philips KMZ10A magneto-resistive sensors) were mounted to a strut fixed to the MTS machine, with one outer and inner pair at 180° and one outer and inner pair at 90°, with each sensor pair using the bracket shown in Figs. 4 and 5 positioned approximately 12.5 mm from the surface of the sidewall with the tire at rest.

With the Conti Sport Contact tire mounted in the MTS Model 860 tread wear machine, lateral force, F_y and Torque, M_y, were varied sinusoidally as shown in Fig. 12, with the lateral force being varied sinusoidally at 0.1667 Hz and the torque being varied sinusoidally at 0.100 Hz. The tire was rotated at a fixed, simulated speed of 50 miles per hour.

Under these circumstances, 30 seconds (750,000 samples) of data, i.e., the circumferential torque, the lateral force, and the vertical force acting on the tire, the inflation pressure, and the raw SWT sensor data, were collected at 25,000 samples per second.

Next, the raw SWT sensor data was processed to calculate the inputs to the neural network, i.e., the phase difference between the two sensor signals in radians, the amplitude of the signal from the outer sensor 26 in millimeters, and the difference in amplitude between the two sensors 26, 28 in millimeters were calculated from the peaks and zero-crossings of the raw SWT sensor data. More specifically, the phase difference was determined using the polynomial fit method described above, the amplitude of the signal from the outer SWT sensor 26 was determined using the peak of the polynomial fit described above, and the difference between the two SWT signal amplitudes was determined using the difference between peaks found using the polynomial fit described above.

Having calculated the phase and two amplitudes, next these input were corrected using the additive correction algorithm described above and both amplitudes were corrected using the multiplicative error correction algorithm described above.

Next, the phase data and two amplitudes were normalized, i.e., scaled to between -1 and +1 by subtracting the maximum value from the minimum value for each parameter, and dividing by the minimum value, and multiplying the resulting value by each data set.

Then the large data set was divided into three sets, i.e., a training set, a validation set, and a test set.

Next, a specific structure was selected for the neural network. For this particular example, a single hidden layer having nine hidden nodes was used, as shown in Fig. 13. A hyperbolic tangent sigmoidal function was used between the inputs and hidden layer. A

linear function was used between the hidden layer and outputs. The "180" in the three inputs (Phase 180, Amp 180 Out, and Amp Delta 180) in Fig. 13 refer to the fact that the sensors 26, 28 were mounted at, and thus the data was collected from, the "12 o'clock" position of the tire, i.e., the top of the tire sidewall as viewed on the vehicle. The 90° data could be used to determine the vertical force, F_z.

Next, the training data set was used to train the neural network with Matlab using the following Matlab neural network object:

```
Neural Network object:

    architecture:

        numInputs: 1
        numLayers: 2
      biasConnect: [1; 1]
     inputConnect: [1; 0]
     layerConnect: [0 0; 1 0]
    outputConnect: [0 1]
    targetConnect: [0 1]

       numOutputs: 1  (read-only)
       numTargets: 1  (read-only)
    numInputDelays: 0  (read-only)
    numLayerDelays: 0  (read-only)

    subobject structures:

            inputs: {1x1 cell} of inputs
            layers: {2x1 cell} of layers
           outputs: {1x2 cell} containing 1 output
           targets: {1x2 cell} containing 1 target
            biases: {2x1 cell} containing 2 biases
      inputWeights: {2x1 cell} containing 1 input weight
      layerWeights: {2x2 cell} containing 1 layer weight

    functions:

          adaptFcn: 'adaptwb'
           initFcn: 'initlay'
        performFcn: 'mse'
          trainFcn: 'trainlm'

    parameters:

        adaptParam: .passes
         initParam: (none)
      performParam: (none)
       trainParam: .epochs, .goal, .max_fail, .mem_reduc,
                   .min_grad, .mu, .mu_dec, .mu_inc,
                   .mu_max, .show, .time

    weight and bias values:

                IW: {2x1 cell} containing 1 input weight matrix
                LW: {2x2 cell} containing 1 layer weight matrix
                 b: {2x1 cell} containing 2 bias vectors
```

```
other:
        userdata: (user stuff)
```

The neural network was trained with Matlab using the Levenberg-Marquardt technique with early stopping. More specifically, the neural network was trained until a validation stop (validation set error increased for five consecutive epochs) occurred at epoch 104. The mean sum of squared errors for the training set at epoch 99 was 0.00176. The mean sum of squared errors for the validation set at epoch 99 was 0.00178.

Using this procedure, the following weights between the inputs and the hidden layer were determined:

	Phase180	Amp180Out	AmpDelta180
H1	7.5750	-0.3542	0.1623
H2	5.1831	-7.7037	-0.7410
H3	-2.4434	5.5960	0.8778
H4	-0.1242	0.9222	-1.3954
H5	5.4329	-7.8189	-1.0483
H6	-0.1375	0.6883	-0.3193
H7	5.6597	3.0346	-0.9307
H8	0.8117	1.3816	-0.5938
H9	1.0578	-1.2053	1.1388

Additionally, the following weights between the hidden layer and the outputs were determined:

	H1	H2	H3	H4	H5	H6	H7	H8	H9
M_y	-0.2718	0.2565	-0.0748	0.2405	-0.2624	-1.2731	0.2896	0.6869	0.7063
F_y	0.5201	-1.3359	0.0085	-1.0817	1.3245	4.5544	-0.1567	-0.1339	0.1094

The following bias weights between the inputs and the hidden layer were determined:

H1	-7.8421
H2	-0.9515

H3	1.5128
H4	-0.1678
H5	-0.9816
H6	-0.7893
H7	-4.8751
H8	0.3697
H9	0.5579

Finally, the following bias weights between the hidden layer and the outputs were determined:

M_y	-1.2825
F_y	3.2547

These particular weights are considered to be valid because the training set, the validation set and the test set all had a mean sum of squared errors that were below 0.002 (all were about 0.00178).

Figures 14 and 15 show a graphical representation of the closeness of the predictions as compared to measured data in the validation set. Using these weights, the lateral force predicted by the neural network is very close to the measured lateral force in the validation set. Similarly, the circumferential torque predicted by the neural network is very close to the measured circumferential torque in the validation set

Example 2 - Bilinear Equations

In this example, the data from Example 1 was used to determine a pair of bilinear equations to predict lateral force and circumferential torque.

The constants for the two equations were calculated with Matlab using the multiple linear least squares regression technique.

Using the above procedure, the following bilinear equations were determined to predict lateral force and circumferential torque:

$$M_y = -5.9835 + 7.4517\,p - 0.7741\,a + 0.3313\,d + 0.7102\,p \cdot a$$

$$F_y = -39.6433 + 7.7312\,p + 6.2483\,a + 9.7848\,d - 2.8222\,p \times a$$

Where,

p = SWT Phase at 180 degree position, in radians

a = SWT Amplitude of outer sensor 26 at 180 degree position, in mm

d = Difference between SWT outer and inner amplitudes, in mm

M_y = Circumferential torque, kN-m

F_y = Lateral Force, kN

Figures 16 and 17 show graphical representations of the closeness of the predictions as compared to measured data in the validation set. Using these bilinear equations, the predicted lateral force is close to the measured lateral force in the validation set. Similarly, the predicted circumferential torque is close to the measured circumferential torque in the validation set. Although the predictions made by the bilinear equations are not as close as the predictions made by the neural network, as can be seen by inspection of Figs. 14-17, the bilinear equations provide reasonably accurate predictions, which can be useful and usable for various applications. Additionally, the greatest deviation between predicted and measured values appears to be when there is no force or torque being applied.

Example 3 - Neural Network

An Contitrac AW P275/65 R17 magnetic sidewall tire was prepared as generally described in U.S. Pat. No. 5,895,854 and copending U.S. Patent Application No. 09/347,757, with 200 phr (parts per hundred) of strontium ferrite powder embedded in the sidewall prior to curing. The embedded strontium ferrite was magnetized to magnetic saturation using 96 electromagnets providing 48 North poles alternating with 48 South poles.

Next, the Contitrac AW P275/65 R17 tire was mounted on an MTS Model 860 tread wear machine (available from MTS Systems Corporation) as follows: The magnetic sidewall tire was mounted to a precision rim. Two pairs of SWT sensors (Philips KMZ10A magneto-resistive sensors) were mounted to a strut fixed to the MTS machine, with one outer and inner pair at 180° and one outer and inner pair at 90°, with each sensor pair using the bracket shown in Figs. 4 and 5 positioned approximately 12.5 mm from the surface of the sidewall with the tire at rest.

With the Contitrac AW P275/65 R17 tire mounted in the MTS Model 860 tread wear machine, vertical force, F_z, lateral force, F_y, and Torque, M_y, were varied sinusoidally similar to Example 1, with the vertical force being varied sinusoidally at 0.25 Hz, the lateral force being varied sinusoidally at 0.15 Hz, and the torque being varied sinusoidally at 0.100 Hz. The tire was rotated at a fixed, simulated speed of 50 miles per hour.

Under these circumstances, 20 seconds (500,000 samples) of data, i.e., the circumferential torque, the lateral force, and the vertical force acting on the tire, the inflation pressure, and the raw SWT sensor data, were collected at 25,000 samples per second.

Next, the raw SWT sensor data was processed to calculate the eight inputs to the neural network, i.e., (1) the phase difference between the two 180° sensor signals in radians (Phase180), (2) the amplitude of the signal from the outer 180° sensor in millimeters (Amp180Out or Amp180), (3) the difference in amplitude between the two 180° sensors in millimeters (AmpDelta180 or Delta180), (4) the phase difference between the two 90° sensor signals in radians (Phase90), (5) the amplitude of the signal from the outer 90° sensor in millimeters (Amp90Out or Amp180), (6) the difference in amplitude between the two 90° sensors in millimeters (AmpDelta90 or Delta90), (7) Phase180 x Amp180Out (after the correction routine was performed) (pxA180), and (8) Phase90 x Amp90Out (after the correction routine was performed) (pxA90) were calculated from the peaks and zero-crossings of the raw SWT sensor data. More specifically, the phase differences were determined using the polynomial fit method described above, the amplitudes of the signals from the outer SWT sensors were determined using the peaks of the polynomial fit described above, and the differences between the two signal amplitudes were determined using the differences between peaks found using the polynomial fit described above.

Having calculated the eight phase and two amplitudes, next these inputs were corrected using the additive correction algorithm described above and both amplitudes were corrected using the multiplicative error correction algorithm described above.

Next, the eight inputs were normalized, i.e., scaled to between -1 and +1 by subtracting the maximum value from the minimum value for each parameter, and diving by the minimum value, and multiplying the resulting value by each data set.

Then the large data set was divided into three sets, i.e., a training set, a validation set, and a test set.

Next, a specific structure was selected for the neural network. For this particular example, a single hidden layer having six hidden nodes was used. A hyperbolic tangent sigmoidal function was used between the inputs and hidden layer. A linear function was used between the hidden layer and outputs.

Next, the training data set was used to train the neural network with Matlab using the following Matlab neural network object:

```
Neural Network object:
```

```
architecture:

          numInputs: 1
          numLayers: 2
        biasConnect: [1; 1]
       inputConnect: [1; 0]
       layerConnect: [0 0; 1 0]
      outputConnect: [0 1]
      targetConnect: [0 1]

         numOutputs: 1  (read-only)
         numTargets: 1  (read-only)
    numInputDelays: 0  (read-only)
    numLayerDelays: 0  (read-only)

    subobject structures:

            inputs: {1x1 cell} of inputs
            layers: {2x1 cell} of layers
           outputs: {1x2 cell} containing 1 output
           targets: {1x2 cell} containing 1 target
            biases: {2x1 cell} containing 2 biases
      inputWeights: {2x1 cell} containing 1 input weight
      layerWeights: {2x2 cell} containing 1 layer weight

    functions:

          adaptFcn: 'adaptwb'
           initFcn: 'initlay'
        performFcn: 'mse'
          trainFcn: 'trainlm'

    parameters:

        adaptParam: .passes
         initParam: (none)
      performParam: (none)
        trainParam: .epochs, .goal, .max_fail, .mem_reduc,
                    .min_grad, .mu, .mu_dec, .mu_inc,
                    .mu_max, .show, .time

    weight and bias values:

                IW: {2x1 cell} containing 1 input weight matrix
                LW: {2x2 cell} containing 1 layer weight matrix
                 b: {2x1 cell} containing 2 bias vectors

    other:
          userdata: (user stuff)
```

The neural network was trained with Matlab using the Levenberg-Marquardt technique with early stopping. More specifically, the neural network was trained until a validation stop (validation set error increased for five consecutive epochs) occurred at epoch 81. The mean sum of squared errors for the training set at epoch 76 was 0.00023. The mean sum of squared errors for the validation set at epoch 76 was 0.0003.

Using this procedure, the following weights between the inputs and the hidden layer were determined:

	Phase180	Amp180	Delta180	Phase90	Amp90	Delta90	pxA180	pxA90
H1	-3.1924	0.1511	-0.2810	0.0578	-2.4559	1.3095	2.6048	-0.1632
H2	0.2276	0.1292	0.0095	-0.0452	-0.1124	0.1021	-0.5314	0.0715
H3	4.0264	-2.7292	6.4593	-1.7411	-0.9765	0.2611	-4.0561	1.8814
H4	-3.4893	1.6882	-0.4483	-0.5887	-0.6309	-0.4819	3.8759	0.3948
H5	0.1973	0.0347	-0.3096	0.2210	-0.4999	0.5343	-0.4009	-0.0815
H6	-0.3868	-1.3459	1.1311	-0.2410	3.6300	-2.9317	0.7292	0.3695

Additionally, the following weights between the hidden layer and the outputs were determined:

	H1	H2	H3	H4	H5	H6
M_y	-0.1101	-3.4672	0.0003	0.0521	0.5608	0.9396
F_y	-0.0784	3.3440	0.0104	-0.5603	-3.7565	0.1112
F_z	-4.7038	8.4356	0.3594	1.6993	11.3365	5.3866

The following bias weights between the inputs and the hidden layer were determined:

H1	1.4653
H2	0.3718
H3	-1.3782
H4	0.5840
H5	0.2758
H6	0.7870

Finally, the following bias weights between the hidden layer and the outputs were determined:

M_y	0.7171
F_y	-0.0399
F_z	-6.2700

These particular weights are considered to be valid because the training set, the validation set and the test set all had a mean sum of squared errors that were below 0.002 (all were about 0.0003 or less).

Figures 18-20 show graphical representations of the closeness of the predictions as compared to measured data in the validation set. Using these weights, the vertical force, lateral force, and circumferential torque predicted by the neural network is nearly identical to the measured values in the validation set.

Example 4 - Bilinear Equations

In this example, the data from Example 2 was used to determine bilinear equations to predict vertical force, lateral force, and circumferential torque.

The constants for the two equations were calculated with Matlab using the multiple linear least squares regression technique.

Using the above procedure, the following bilinear equations were determined to predict vertical force, lateral force, and circumferential torque:

F_y = -12.9336 + -11.9139 p180 - 4.4413 a180 + 9.9952 d180 - 5.7197 p90 + 4.1038 a90 - 5.5416 d90 + 0.1871 (p180 x a180) + 0.0676 (p90 x a90)

F_z = 8.6908 - 79.1627 p180 - 1.1944 a180 + 1.4968 d180 + 10.8531 p90 + 1.2659 a90 + 0.0597 d90 + 3.5677 (p180 x a180) + 0.7880(p90 x a90)

M_y = -0.9059 + 6.5357 p180 - 0.6891 a180 + 1.6094 d180 + 0.0920 p90 + 0.4191 a90 - 0.6654 d90 + 0.3710 (p180 x a180) - 0.0027 (p90 x a90)

Where,

p180 = SWT Phase at 180 degree position, radians
a180 = SWT Amplitude of outer sensor at 180 degree position, mm
d180 = Difference between SWT outer and inner amplitudes at 180 degrees, mm
p90 = SWT Phase at 90 degree position, radians
a90 = SWT Amplitude of outer sensor at 90 degree position, mm
d90 = Difference between SWT outer and inner amplitudes at 90 degrees, mm

F_y = Lateral force in kN
F_z = Vertical (Normal) force in kN
M_y = Circumferential torque, kN-m

Figures 22-24 show graphical representations of the closeness of the predictions as compared to measured data in the validation set. Using these bilinear equations, the predicted vertical force, lateral force, and circumferential torque are very close to the measured values. Although the predictions made by the bilinear equations are not as close as the predictions

made by the neural network, with the additional sensor pair, the bilinear equations in this example provide very accurate predictions, which can be useful and usable for many applications.

An additional example is attached hereto as Appendix 1 and incorporated herein by reference.

Referring back to Figure 2, as mentioned above, exemplary control units 32 benefiting from the present invention include but are not limited to ABS control units, traction control system (TCS) control units, electronic stability control (ESC) control units, integrated vehicle dynamics (IVD)) control units, locked differential control units, suspension control units, brake assist control units, intelligent cruise control units, steering assist control units, deflation detection control units, navigation control units, rollover prevention control units, and a brake-by-wire control units.

ABS control units can benefit from the present invention in at least two ways. First, the present invention can be used to reduce ABS chattering. ABS chattering typically results from the nature of slip data. Force data provided by the present invention is smoother than slip data. Accordingly, an ABS controller using force data taken in accordance with the present invention will have less chattering.

Also, ABS control units can be made safer using the lateral force predicted by the present invention. Referring now to Figure 18, a series of μ-slip curves at various steering angles (α) are shown. No steering results in no lateral force. Curve 200 is a typical μ-slip curve showing longitudinal force (i.e., braking force) F_x at a steering angle of 0 , i.e., under no lateral force. As shown by that curve 200 and as known to those in the art, the peak of that curve 200 is at a point 202 at about 13% slip. As also known to those in the art, it is desirable for an ABS control unit to strive to control the slip to provide peak braking force at about 10% slip or so.

A steering motion causes a tire to rotate, which induces a lateral force on the tire. Curves 210 and 220 in Figure 18 are μ-slip curves showing longitudinal force F_x at a steering angle of 5 and 10 , respectively. The corresponding lateral forces F_y are also shown. The peak of curve 210 is at a point 212 at about 20% slip and the peak of curve 220 is at a point 222 at about 32% slip. That is, a lateral force on the tire, as caused by a steering maneuver, causes the peak of the μ-slip curve to be moved.

The effect of this should be apparent. An ABS control unit incapable of detecting lateral force would strive to control the slip at about 10% slip or so, which would be effective for maximum braking force as long as there is no steering action. However, a slip at around 10% is not at the peak of the curves 210 and 220. Therefore, a steering maneuver would confound the ABS control unit incapable of detecting lateral force, rendering it incapable of generating a maximum braking force.

On the other hand, an ABS controller 32 modified to accept a predicted lateral force from a force prediction unit 22 of the present invention (or even implemented with the same processor) could vary the slip control point in accordance with the predicted lateral force to provide maximum braking force. For example, the ABS control unit 32 could be modified to select a μ-slip curve or other control parameter based on the predicted lateral force from the force prediction unit 22. In the context of Figure 18 a first predicted lateral force would be used to trigger curve 210 to be used, and the ABS control unit 32 would tend to control the slip at about point 212 to provide maximum braking. A different, greater predicted lateral force would be used to trigger curve 220 to be used, and the ABS control unit 32 would then tend to control the slip at about point 222 to provide maximum braking. Changing the prediction of lateral force at any instant would change the μ-slip curve used the next instant. Although only three μ-slip curves are described in this example, one of ordinary skill in the art would understand that more curves could be used, or the lateral force (or some other parameter determined by the force prediction unit 22) could be used in an equation or set of equations by the ABS control unit 32 to vary the slip control point in accordance with the predicted lateral force.

While the present invention has been illustrated by the description of embodiments thereof, and while the embodiments have been described in considerable detail, it is not the intention of the applicant to restrict or in any way limit the scope of the appended claims to such detail. Additional advantages and modifications will readily appear to those skilled in the art. For example, the SWT sensors described herein have an analog current output; in the alternative, sensors having outputs in the frequency domain might be used in a system made in accordance with the teachings of the present invention. In addition, the SWT sensors described herein are magnetic sensors; other sidewall torsion sensors might be used in a system made in accordance with the teachings of the present invention. Therefore, the invention in its broader aspects is not limited to the specific details, representative apparatus and method, and illustrative examples

shown and described. Accordingly, departures may be made from such details without departing from the spirit or scope of the applicant's general inventive concept.

Continental®

GENERAL TIRE

TO:

FROM: J. M. Giustino
Test Development

DATE:

SUBJECT: Measurement of Lateral Force and Longitudinal Torque Using SWT Sensors

Objective

To develop an algorithm to predict lateral force and longitudinal torque from measurements taken using the tire sidewall sensoric system (SWT).

Summary

A 1997 Ford Taurus was equipped with an instrumented hub to measure the tangential, lateral and normal forces along with the longitudinal torque generated in the contact patch by the front left tire. The Taurus was also equipped with an SWT system, modified to record the raw waveforms of the sensors. The Taurus tire, built at Charlotte, contained a two mm thick sidewall veneer compound filled with iron oxide particles that were magnetized to provide a magnetic field consisting of 32 nominally equally spaced "poles" per revolution. A computer program was written to record the three forces and torque along with the SWT sensor waveforms. Artificial neural networks (ANNs) were trained to predict the longitudinal torque and lateral force as outputs using the SWT sensor data as inputs. The ANN algorithms resulted in high correlation coefficients (R-values) between the predicted and measured longitudinal torque and lateral force (exceeding 0.95).

Conclusions

- Both longitudinal torque and lateral force may be measured using the SWT system along with appropriately trained ANNs.

Appendix 1

Measurement of Lateral Force and Longitudinal Torque Using SWT Sensors

Introduction

The primary function of the sidewall torsion sensor system (SWT) is to measure the torsional deformation (in the tangential direction) of the tire and calculate the applied driving or braking torque. As described in reference [1], however, the application of lateral forces on the tire confounds the measurement of longitudinal torque using the SWT sensors as originally envisioned. Thus, cornering maneuvers would adversely affect the calculation of driving or braking torque and limit the usefulness of the SWT system. The purpose of this report is to describe a technique not only for decoupling the lateral and tangential forces, but also to predict the lateral force acting on the tire using the SWT sensors.

The technique involves the use of artificial neural network (ANN) computer algorithms. The architecture of the ANN was a Multilayer Perceptron (MLP) consisting of one input, one hidden and one output layer [2]. Data derived from the raw waveforms of the SWT sensors were used as inputs into the ANN, while longitudinal torque and lateral force measured with an instrumented hub were used as the outputs. The number of nodes (or neurons) in the hidden layer were typically five to twenty. A nonlinear, hyperbolic tangent sigmoidal transfer function was used between the input and hidden layers, while both linear and hyperbolic tangent transfer functions were evaluated between the hidden and output layers.

In order to obtain the input and output data, a data acquisition computer program was written using LABVIEW to record the raw waveforms from the SWT sensors and the forces and torques measured by the instrumented hub mounted at the left front wheel position of a 1997 Ford Taurus. The data were then reduced further using routines written in MATLAB.

Experimental Tests

The National Instruments data acquisition card used in the experiments was capable of collecting one channel of data at a rate of 1.1 mega samples per second. For these tests, seven channels of data were collected at 50,000 samples per second. Two of the channels were the raw waveforms from the upper and lower SWT sensors (i.e., the sensor near the tread and the sensor near the bead). The other four channels collected the tangential, lateral and normal forces and the longitudinal torque from the instrumented hub. The computer was a "luggable" PC (Dolch) containing a 166 MHz Pentium chip with 128 megabytes of RAM and two gigabytes of hard disk space. The front passenger seat was removed from the Taurus, and a rack for holding the computer was mounted in its place. The computer, with its detachable keyboard, was operated from the right back seat.

The tire was a P205/70 R15 constructed with a 2-mm veneer of a sidewall compound containing 200 phr of iron oxide. The veneer was hand constructed from 32 individual strips of compound that were magnetized with Charlotte's lab equipment prior to placing it on the green tire and curing. Adjacent north poles were placed next to each other so that there were 32 equally spaced north to north and south to south "poles" providing a quasi sinewave with 32 crests and 32 valleys per tire revolution in the waveform produced from the SWT sensors.

The tire and instrumented hub were mounted on a 1997 Taurus that was equipped with an SWT sensor system modified to record the raw waveforms from the sensors. Figures 1 and 2 show the instrumented hub and SWT sensors mounted on the Taurus.

Measurement of Lateral Force and Longitudinal Torque Using SWT Sensors

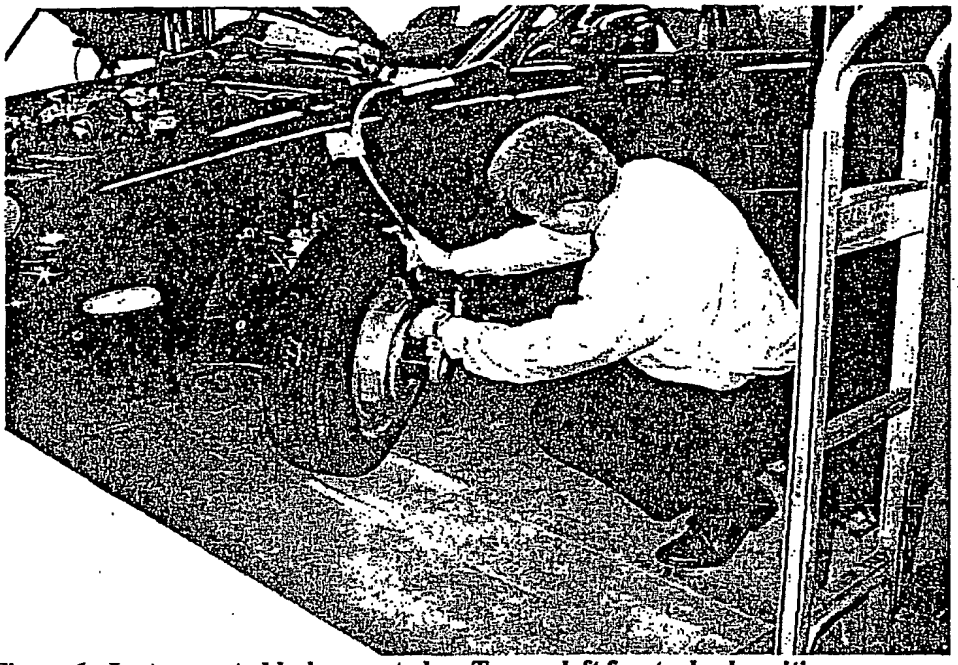

Figure 1. Instrumented hub mounted on Taurus left front wheel position.

Driving tests included constant speed followed by braking and accelerating maneuvers to provide the longitudinal torque and S-turn maneuvers at constant speed to provide the lateral force. Other tests included S-turn maneuvers with braking and acceleration to provide a combination of longitudinal torque and lateral forces. Figure 3 shows the data acquisition screen after taking data from a test that involved a constant speed followed by a braking and then an accelerating maneuver. The forces and torque are shown in the upper window while the SWT signals are shown in the lower window. In this example, a fairly constant, zero lateral force was maintained by driving straight ahead. (Fx, Fy and Fz represent the tangential, lateral and normal forces while My represents the circumferential torque). The data

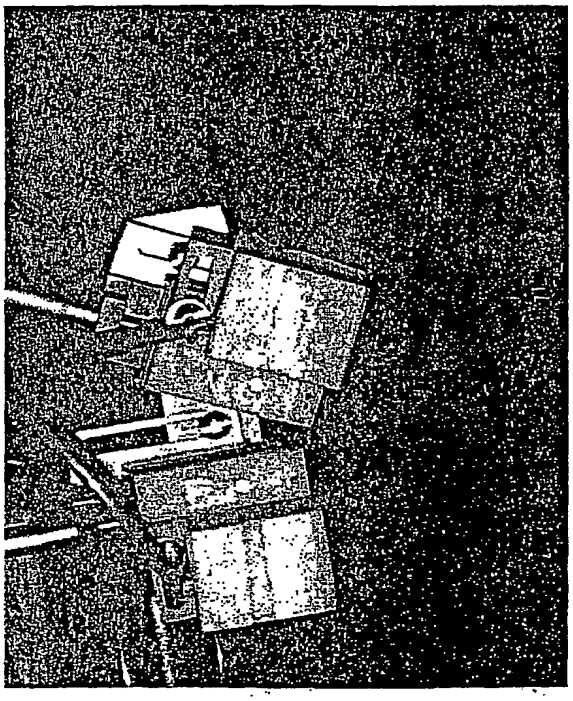

Figure 2. SWT sensors mounted on Taurus

Measurement of Lateral Force and Longitudinal Torque Using SWT Sensors

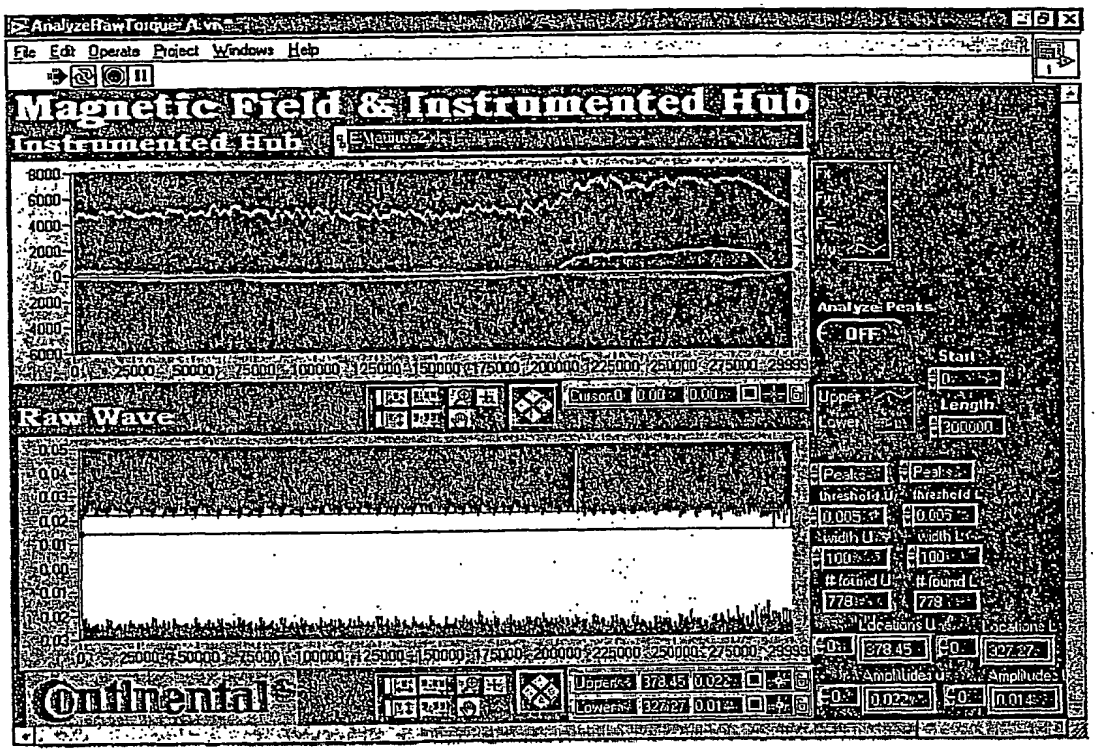

Figure 3. Data acquisition screen. All 300,000 points of data collected at 50,000 samples per second. Upper (right) curves, from top to bottom: Fz, My, Fy, Fx. Forces in Newtons, N, torque in N-m. Lower curves: Upper and lower sensors. Amplitude in volts.

acquisition program also was programmed to pick the locations and amplitudes of the peaks or valleys of the SWT signals and the corresponding data from the forces and torque. Polynomials fitted to each peak were differentiated to determine their maxima and corresponding times the maxima occurred. For each SWT sensor, the periods between pulses were calculated using these peak times. By comparing adjacent times from the upper and lower SWT sensors, the phase differences were calculated. The ratio of the phase difference to the lower SWT sensor period is proportional to the longitudinal torsion of the sidewall, as described in [1]. The peak SWT amplitudes from the upper and lower sensors, the period of the lower sensor and the ratio were used as inputs for the ANN described below. The corresponding longitudinal torque and lateral force were used as the output.

Measurement of Lateral Force and Longitudinal Torque Using ... Sensors

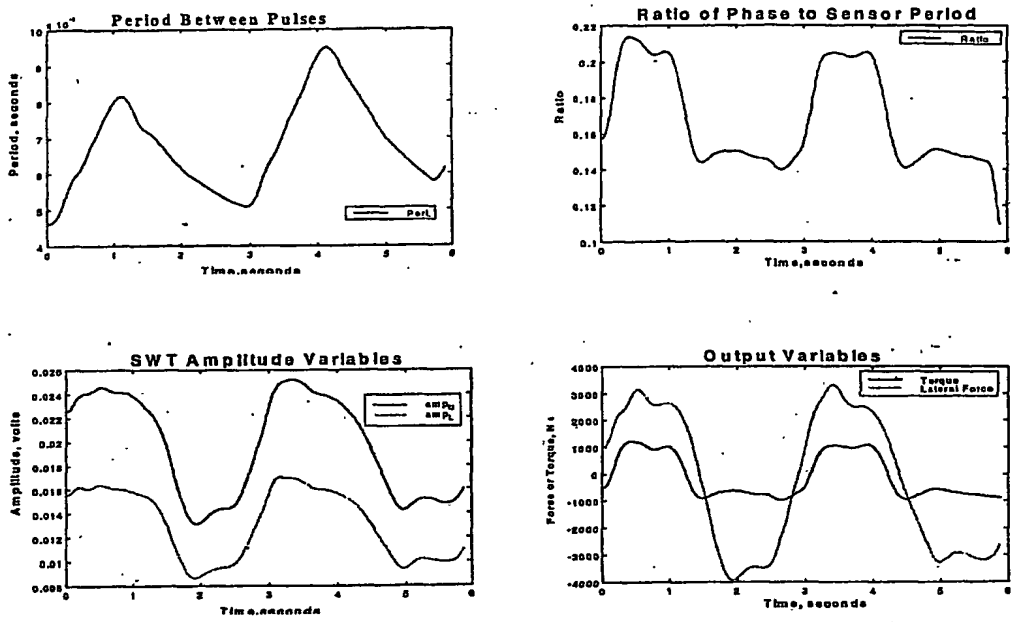

Figure 4. The input and output data smoothed using a moving average filter corresponding to one tire revolution.

Analysis

The objective of the analysis was to predict longitudinal torque and lateral force from the data generated by the SWT sensors. However, previous analyses had shown that the longitudinal torque and lateral forces were confounded. That is, the longitudinal torque measured using the original SWT system was incorrect during cornering maneuvers generating large lateral forces. Familiarity with Pajecka's "magic" formula [3] that relates forces and torques generated in the tire contact patch under various conditions of braking torque, camber and slip angles suggested that the coupling of the two forces is not simple or linear. A technique for decoupling the forces was needed.

Mathematically, the problem was to create a mapping function from an input space (the measurements made using the SWT sensors) to an output space (measurements of torque and lateral force made using the instrumented hub). This type of problem may be solved using artificial neural networks, especially those involving Multilayer Perceptrons (MLP) [4]. Figure 4 shows the input and output variables plotted versus time after passing them through a 32 point moving average filter (equivalent to one tire revolution). Figure 5 shows the architecture of one artificial neural net that was used to predict the longitudinal torque from the input variables - Amp_L, Amp_U, Per_L, and ratio representing the lower and upper SWT sensor peak amplitudes in volts, the periods of the lower sensor in seconds and the ratio, respectively. This three layer MLP had four nodes in the input layer, twelve nodes in the hidden layer, and one node in the output layer. Non-linear, hyperbolic tangent, sigmoidal transfer functions were used between the input and hidden layers, while linear transfer functions were used between the hidden and output layers.

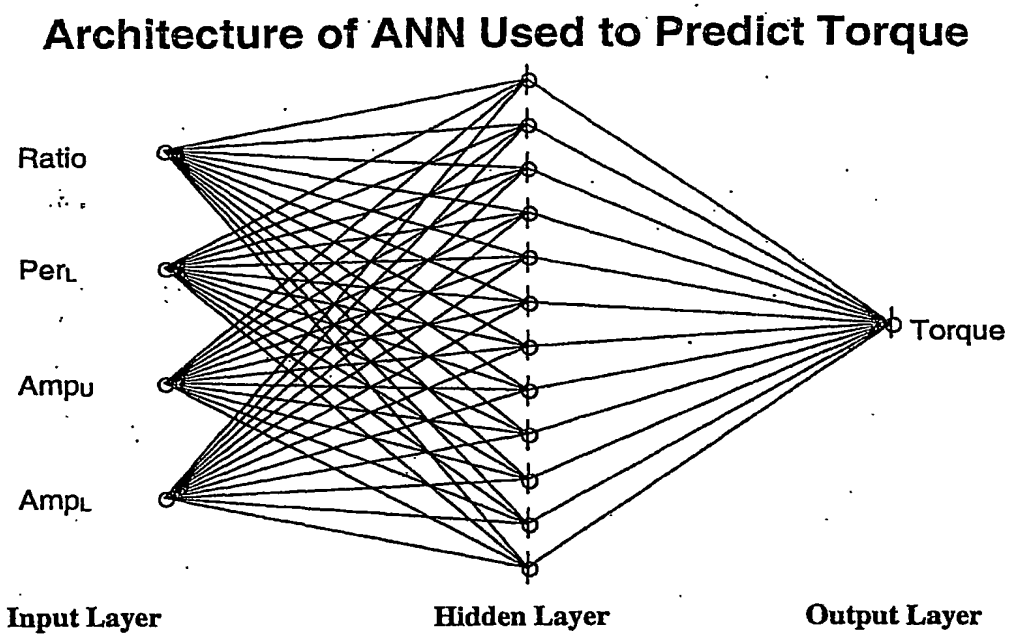

Figure 5. Example of a neural network model used to predict the longitudinal torque from the measurements made using the SWT sensors.

The networks were trained using Levenberg-Marquardt methods. The ANN model in figure 5 was chosen using several model selection criteria. The problem is that if the model is too flexible (i.e., it has too many hidden neurons, or too many input variables or is "overtrained"), it will fit the noise, if it is too inflexible it will miss the target. To prevent "overtraining" or "overfitting" in which the network is trained to very low errors causing the network to "learn" all of the peculiarities of the data including noise of the training data set, "early stopping" was employed to limit the number of training epochs. Data from two-thirds of the test run were used as a training set, while the other third of the data were used as a cross validation set (i.e., every third point was taken as a validation point). In addition, the leave one out (LOO) cross-validation and Akaike's final prediction error (fpe) were used. All of these techniques estimate the prediction error, i.e., they estimate how well the trained model will perform on future (unknown) inputs (how well the model "generalizes"). Software written in MATLAB (based on reference [2]) semi-automated the model selection criteria. Plots of prediction error (early stopping, LOO and fpe) versus training epoch number were generated for models starting with one neuron in the hidden layer up to any desired number (usually about twenty). Figure 6 shows the results for the model shown in figure 5. In addition to these techniques, weight decay or "regularization" was employed to prevent the weights (coefficients of the model) from growing rapidly, a technique that improves the ability of the model to generalize. (The regularization parameter is shown as the variable D in figure 6 – a two element vector denoting the value used between the input and hidden layers and the value between the hidden and output layers).

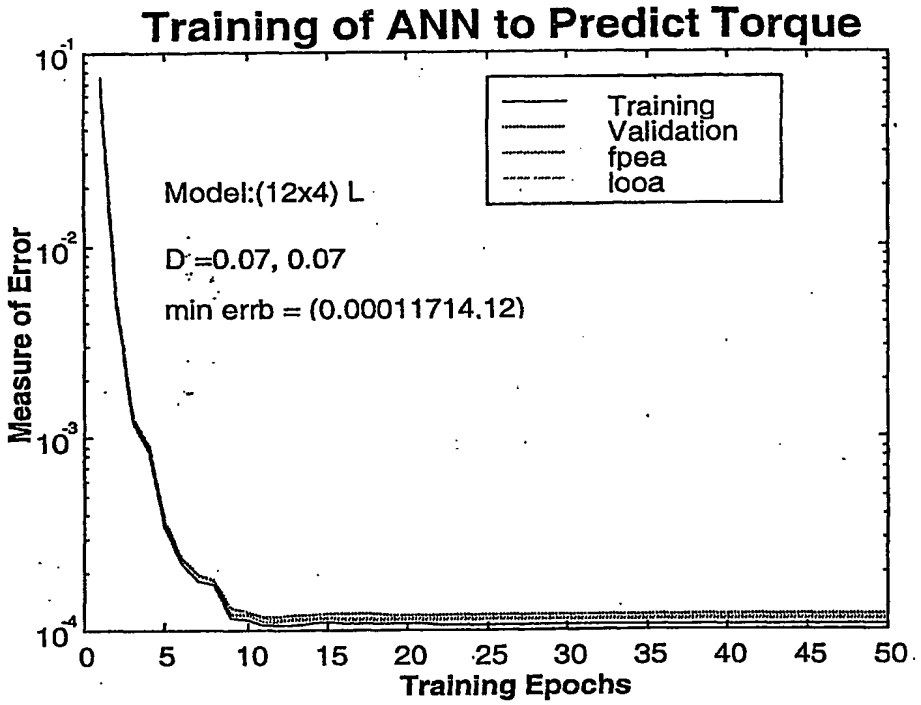

Figure 6. Model selection criteria for the model shown in figure 5. The cross-validation error (0.000117) and training epoch number (12) is represented by min errb. Also shown are the leave one out and final prediction errors along with the training set error. The model consisted of 12 neurons in the hidden layer and 4 in the input layer with a linear connection between the hidden and output layers (12x4)L. D is the vector of "regularization" parameters for the connections from input to hidden and hidden to output layers.

Results

The left-hand plots in figure 7 show the correlations between calculated and measured longintudinal torque and lateral force that resulted from the ANNs. Both the training and validation data sets are plotted. The correlation coefficient was 0.9997 for the calculated and measured longitudinal torque, while it was 0.9996 for the calculated and predicted lateral force. The standard errors of the predictions were 17.73 N-m and 73.7 N for the longitudinal torque and lateral force, respectively. The right hand plots in figure 7 compare the calculated versus measured longitudinal torque and lateral force versus time in seconds.

Measurement of Lateral Force and Longitudinal Torque Using ..../T Sensors

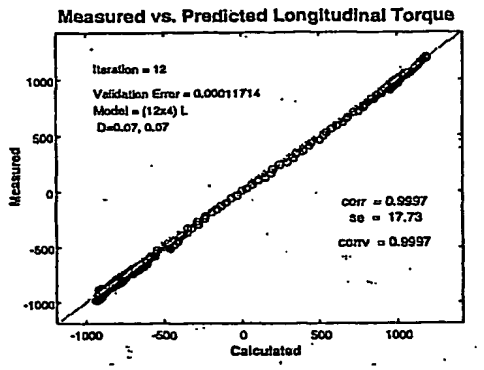

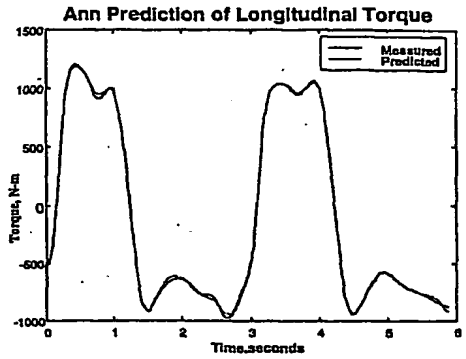

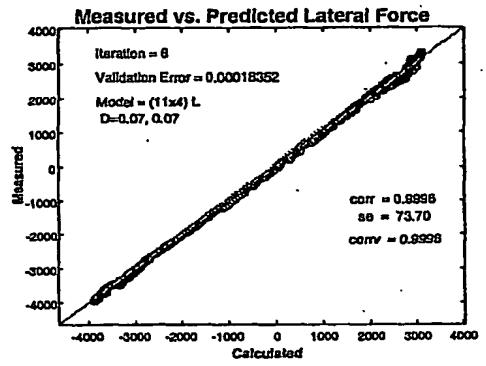

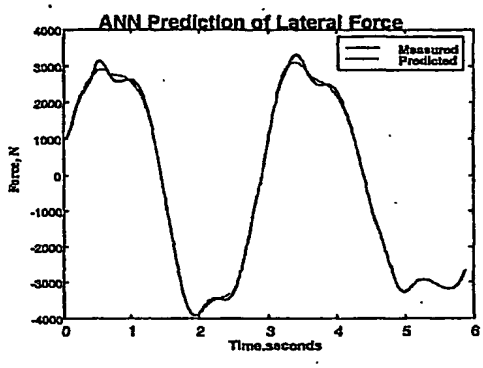

Measurement of Lateral Force and Longitudinal Torque Using ... Γ Sensors

References

1. Becherer, Thomas, *Status report SWT-Sensor*, Continental Aktiengesellschaft, November 27, 1996.
2. M. Nørgaard, *Neural Network Based System Identification Toolbox*, Tech. Report. 95-E-773, Institute of Automation, Technical University of Denmark, 1995.
3. Pacejka, "magic formula" reference.
4. M. Smith, Neural Networks for Statistical Modeling, Van Nostrand Reinhold, New York, 1993, ISBN 0-442-01310-8.
5. Sarle, W.S., ed. (1997), Neural Network FAQ, part 1 of 7: Introduction, periodic posting to the Usenet newsgroup comp.ai.neural-nets, URL: ftp://ftp.sas.com/pub/neural/FAQ.html

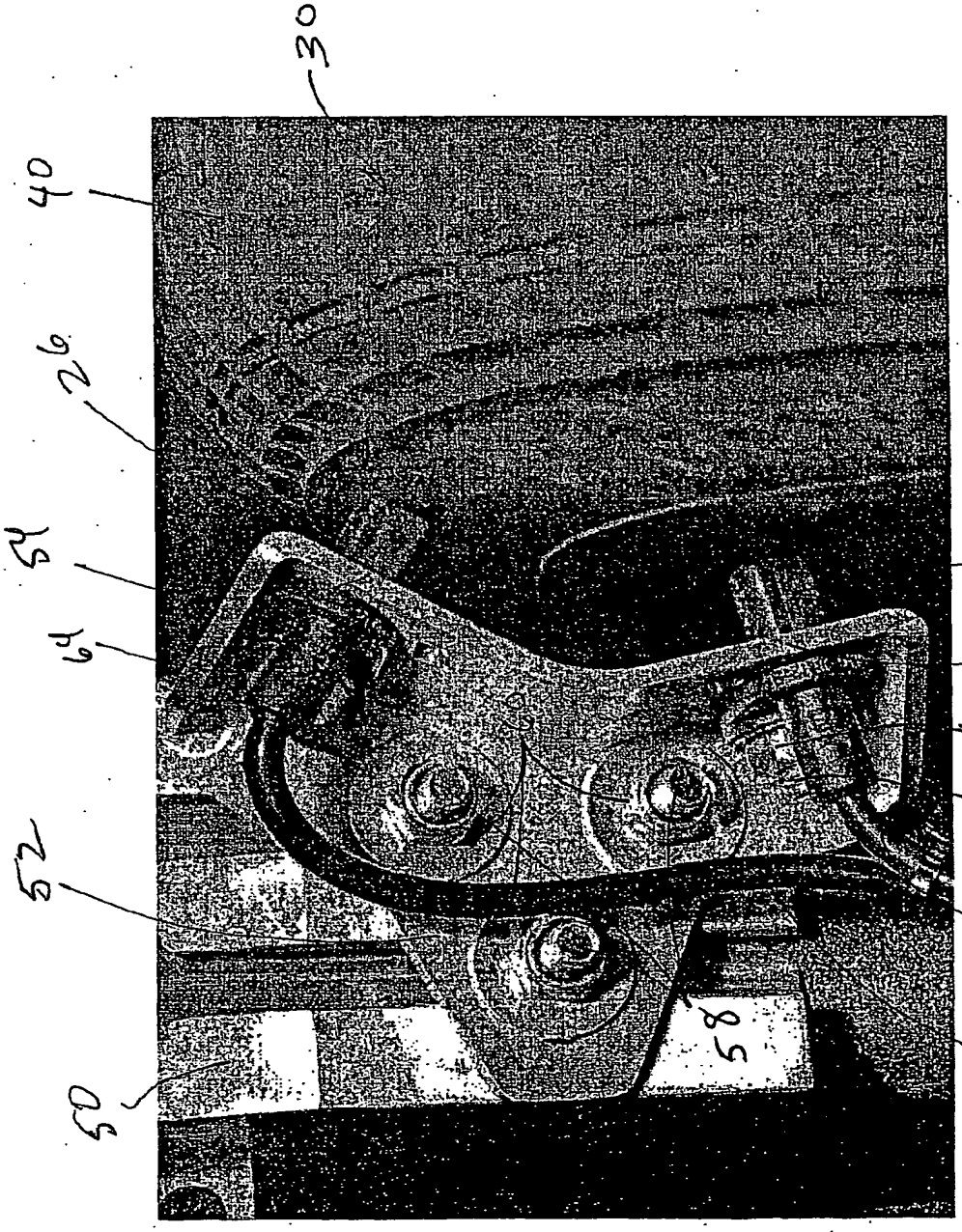

Fig. 5

Appendix 2

I claim:

1. A vehicle control system, comprising: a force prediction unit for being placed in circuit communication with a tire deformation sensor and at least one other sensor, receiving a tire deformation input from the tire deformation sensor, and receiving at least one other tire sensor input from the at least one other sensor, said force prediction unit comprising a preprogrammed processor receiving the tire deformation input and the at least one other sensor input, said force prediction unit characterized by implementing preprogrammed equations having constants determined from previously collected data to determine from at least the tire deformation input and the at least one other sensor input an output corresponding to a predicted circumferential torque or longitudinal force acting on a tire.

2. The vehicle control system of claim 1, wherein said preprogrammed processor of said force prediction unit executes code implementing a neural network trained with previously collected data to determine from at least the tire deformation input and the at least one other sensor input an output corresponding to a predicted circumferential torque or longitudinal force acting on the tire.

3. The vehicle control system of claim 1, wherein said preprogrammed processor of said force prediction unit executes code implementing a multi-layer neural network trained with previously collected data to determine from at least the tire deformation input and the at least one other sensor input an output corresponding to a predicted circumferential torque or longitudinal force acting on the tire, said multi-layer neural network having an input layer, at least one hidden layer, and an output layer.

4. The vehicle control system of claim 3, wherein said preprogrammed processor implements equations between said input layer and said at least one hidden layer in the form of a hyperbolic tangent sigmoidal transfer function, and wherein said preprogrammed processor implements equations between said hidden layer and said output layer in the form of a linear function.

5. The vehicle control system of claim 1, wherein said preprogrammed processor of said force prediction unit executes code implementing an equation using constants determined using multiple-linear-least squares regression analysis of previously collected data to determine from at least the tire deformation input and the at least one other sensor input an output corresponding to a predicted circumferential torque or longitudinal force acting on the tire.

6. The vehicle control system of claim 5, wherein the equation implemented by the preprogrammed processor of said force prediction unit is a bilinear equation.

7. The vehicle control system of claim 1, wherein said the tire deformation input and the at least one other sensor input comprise (a) a phase input related to a phase difference between the at least two sensors and indicative of torsional deformation of the tire and (b) an amplitude input related to a distance between the tire sidewall and the tire deformation sensor and indicative of a force acting on the tire, said preprogrammed processor accepting as inputs the phase input and the amplitude input and using at least the phase input and amplitude input to determine at least an output corresponding to a predicted circumferential torque or longitudinal force acting on the tire.

8. The vehicle control system of claim 2, wherein said the tire deformation input and the at least one other sensor input comprise (a) a phase input related to a phase difference between the at least two sensors and indicative of torsional deformation of the tire and (b) an amplitude input related to a distance between the tire sidewall and the tire deformation sensor and indicative of a force acting on the tire, said neural network accepting as inputs the phase input and the amplitude input and using at least the phase input and amplitude input to determine at least an output corresponding to a predicted circumferential torque or longitudinal force acting on the tire.

9. The vehicle control system of claim 6, wherein said the tire deformation input and the at least one other sensor input comprise (a) a phase input related to a phase difference between the at least two sensors and indicative of torsional deformation of the tire and (b) an amplitude input related to a distance between the tire sidewall and the tire deformation sensor and indicative of a force acting on the tire, said bilinear equation being a function of at least the phase input and the amplitude input to determine an output corresponding to a predicted circumferential torque or longitudinal force acting on the tire.

10. The vehicle control system of any of claims 1-9, wherein the tire deformation sensor comprises a magnetic tire sidewall torsion (SWT) sensor, said SWT sensor including a magnetic sensor positioned proximate to a sidewall of the tire that has been magnetized with alternating magnetic poles.

11. A vehicle control system, comprising: a force prediction unit for being placed in circuit communication with a tire deformation sensor and at least one other sensor, receiving a tire deformation input from the tire deformation sensor, and receiving at least one other tire sensor input from the at least one other sensor, said force prediction unit comprising a preprogrammed processor receiving the tire deformation input and the at least one other sensor input, said force prediction unit characterized by implementing preprogrammed equations having constants determined from previously collected data to determine from at least the tire deformation input and the at least one other sensor input an output corresponding to a predicted lateral force acting on a tire.

12. The vehicle control system of claim 11, wherein said preprogrammed processor of said force prediction unit executes code implementing a neural network trained with previously collected data to determine from at least the tire deformation input and the at least one other sensor input an output corresponding to a predicted lateral force acting on the tire.

13. The vehicle control system of claim 11, wherein said preprogrammed processor of said force prediction unit executes code implementing a multi-layer neural network trained with previously collected data to determine from at least the tire deformation input and the at least one other sensor input an output corresponding to a predicted lateral force acting on the tire, said multi-layer neural network having an input layer, at least one hidden layer, and an output layer.

14. The vehicle control system of claim 13, wherein said preprogrammed processor implements equations between said input layer and said at least one hidden layer in the form of a hyperbolic tangent sigmoidal transfer function, and wherein said preprogrammed processor implements equations between said hidden layer and said output layer in the form of a linear function.

15. The vehicle control system of claim 11, wherein said preprogrammed processor of said force prediction unit executes code implementing an equation using constants determined using multiple-linear-least squares regression analysis of previously collected data to determine from at least the tire deformation input and the at least one other sensor input an output corresponding to a predicted lateral force acting on the tire.

16. The vehicle control system of claim 15, wherein the equation implemented by the preprogrammed processor of said force prediction unit is a bilinear equation.

17. The vehicle control system of claim 11, wherein said the tire deformation input and the at least one other sensor input comprise (a) a phase input related to a phase difference between the at least two sensors and indicative of torsional deformation of the tire and (b) an amplitude input related to a distance between the tire sidewall and the tire deformation sensor and indicative of a force acting on the tire, said preprogrammed processor accepting as inputs the phase input and the amplitude input and using at least the phase input and amplitude input to determine at least an output corresponding to a predicted lateral force acting on the tire.

18. The vehicle control system of claim 12, wherein said the tire deformation input and the at least one other sensor input comprise (a) a phase input related to a phase difference between the at least two sensors and indicative of torsional deformation of the tire and (b) an amplitude input related to a distance between the tire sidewall and the tire deformation sensor and indicative of a force acting on the tire, said neural network accepting as inputs the phase input and the amplitude input and using at least the phase input and amplitude input to determine at least an output corresponding to a predicted lateral force acting on the tire.

19. The vehicle control system of claim 16, wherein said the tire deformation input and the at least one other sensor input comprise (a) a phase input related to a phase difference between the at least two sensors and indicative of torsional deformation of the tire and (b) an amplitude input related to a distance between the tire sidewall and the tire deformation sensor and indicative of a force acting on the tire, said bilinear equation being a function of at least the phase input and the amplitude input to determine an output corresponding to a predicted lateral force acting on the tire.

20. The vehicle control system of any of claims 11-19, wherein the tire deformation sensor comprises a magnetic tire sidewall torsion (SWT) sensor, said SWT sensor including a magnetic sensor positioned proximate to a sidewall of the tire that has been magnetized with alternating magnetic poles.

21. A vehicle control system, comprising: a force prediction unit for being placed in circuit communication with a tire deformation sensor and at least one other sensor, receiving a tire deformation input from the tire deformation sensor, and receiving at least one other tire sensor input from the at least one other sensor, said force prediction unit comprising a preprogrammed processor receiving the tire deformation input and the at least one other sensor input, said force

prediction unit characterized by implementing preprogrammed equations having constants determined from previously collected data to determine from at least the tire deformation input and the at least one other sensor input an output corresponding to a predicted vertical force acting on a tire.

22. The vehicle control system of claim 21, wherein said preprogrammed processor of said force prediction unit executes code implementing a neural network trained with previously collected data to determine from at least the tire deformation input and the at least one other sensor input an output corresponding to a predicted vertical force acting on the tire.

23. The vehicle control system of claim 21, wherein said preprogrammed processor of said force prediction unit executes code implementing a multi-layer neural network trained with previously collected data to determine from at least the tire deformation input and the at least one other sensor input an output corresponding to a predicted vertical force acting on the tire, said multi-layer neural network having an input layer, at least one hidden layer, and an output layer.

24. The vehicle control system of claim 23, wherein said preprogrammed processor implements equations between said input layer and said at least one hidden layer in the form of a hyperbolic tangent sigmoidal transfer function, and wherein said preprogrammed processor implements equations between said hidden layer and said output layer in the form of a linear function.

25. The vehicle control system of claim 21, wherein said preprogrammed processor of said force prediction unit executes code implementing an equation using constants determined using multiple-linear-least squares regression analysis of previously collected data to determine from at least the tire deformation input and the at least one other sensor input an output corresponding to a predicted vertical force acting on the tire.

26. The vehicle control system of claim 25, wherein the equation implemented by the preprogrammed processor of said force prediction unit is a bilinear equation.

27. The vehicle control system of claim 21, wherein said the tire deformation input and the at least one other sensor input comprise (a) a phase input related to a phase difference between the at least two sensors and indicative of torsional deformation of the tire and (b) an amplitude input related to a distance between the tire sidewall and the tire deformation sensor and indicative of a

force acting on the tire, said preprogrammed processor accepting as inputs the phase input and the amplitude input and using at least the phase input and amplitude input to determine at least an output corresponding to a predicted vertical force acting on the tire.

28. The vehicle control system of claim 22, wherein said the tire deformation input and the at least one other sensor input comprise (a) a phase input related to a phase difference between the at least two sensors and indicative of torsional deformation of the tire and (b) an amplitude input related to a distance between the tire sidewall and the tire deformation sensor and indicative of a force acting on the tire, said neural network accepting as inputs the phase input and the amplitude input and using at least the phase input and amplitude input to determine at least an output corresponding to a predicted vertical force acting on the tire.

29. The vehicle control system of claim 26, wherein said the tire deformation input and the at least one other sensor input comprise (a) a phase input related to a phase difference between the at least two sensors and indicative of torsional deformation of the tire and (b) an amplitude input related to a distance between the tire sidewall and the tire deformation sensor and indicative of a force acting on the tire, said bilinear equation being a function of at least the phase input and the amplitude input to determine an output corresponding to a predicted vertical force acting on the tire.

30. The vehicle control system of any of claims 21-29, wherein the tire deformation sensor comprises a magnetic tire sidewall torsion (SWT) sensor, said SWT sensor including a magnetic sensor positioned proximate to a sidewall of the tire that has been magnetized with alternating magnetic poles.

31. The vehicle control system of claim 1, wherein said force prediction unit is further characterized by implementing preprogrammed equations having constants determined from previously collected data to determine from at least the tire deformation input and the at least one other sensor input (a) an output corresponding to a predicted circumferential torque or longitudinal force acting on the tire and (b) an output corresponding to a predicted force acting on the tire that is skewed with respect to the longitudinal force acting on the tire.

32. The vehicle control system of claim 31, wherein said force prediction unit is further characterized by implementing preprogrammed equations having constants determined from previously collected data to determine from at least the tire deformation input and the at least

one other sensor input (a) an output corresponding to a predicted circumferential torque or longitudinal force acting on the tire and (b) an output corresponding to a predicted lateral force acting on the tire.

33. The vehicle control system of claim 31, wherein said force prediction unit is further characterized by implementing preprogrammed equations having constants determined from previously collected data to determine from at least the tire deformation input and the at least one other sensor input (a) an output corresponding to a predicted circumferential torque or longitudinal force acting on the tire and (b) an output corresponding to a predicted vertical force acting on the tire.

34. The vehicle control system of claim 10, wherein said force prediction unit is further characterized by implementing preprogrammed equations having constants determined from previously collected data to determine from at least the tire deformation input and the at least one other sensor input (a) an output corresponding to a predicted lateral force acting on the tire and (b) an output corresponding to a predicted force acting on the tire that is skewed with respect to the lateral force acting on the tire.

35. The vehicle control system of claim 34, wherein said force prediction unit is further characterized by implementing preprogrammed equations having constants determined from previously collected data to determine from at least the tire deformation input and the at least one other sensor input (a) an output corresponding to a predicted lateral force acting on the tire and (b) an output corresponding to a predicted vertical force acting on the tire.

36. The vehicle control system of claim 20, wherein said force prediction unit is further characterized by implementing preprogrammed equations having constants determined from previously collected data to determine from at least the tire deformation input and the at least one other sensor input (a) an output corresponding to a predicted vertical force acting on the tire and (b) an output corresponding to a predicted force acting on the tire that is skewed with respect to the vertical force acting on the tire.

37. A vehicle control system comprising:

(a) a force prediction unit for being placed in circuit communication with a tire deformation sensor and at least one other sensor, receiving a tire deformation input from the tire deformation sensor, and receiving at least one other tire sensor input from the at

least one other sensor, said force prediction unit comprising a preprogrammed processor receiving the tire deformation input and the at least one other sensor input, said force prediction unit characterized by implementing preprogrammed equations having constants determined from previously collected data to determine from at least the tire deformation input and the at least one other sensor input an output corresponding to a predicted circumferential torque or longitudinal force acting on a tire and outputting a predicted circumferential torque or longitudinal force output corresponding to the predicted circumferential torque or longitudinal force acting on the tire; and

(b) a control unit in circuit communication with said force prediction unit for receiving the predicted circumferential torque or longitudinal force output and for being placed in circuit communication with vehicle actuators, said control unit characterized by altering the dynamic state of the vehicle via the actuators responsive at least in part to the predicted circumferential torque or longitudinal force output from the force prediction unit.

38. A vehicle control system comprising:

(a) a force prediction unit for being placed in circuit communication with a tire deformation sensor and at least one other sensor, receiving a tire deformation input from the tire deformation sensor, and receiving at least one other tire sensor input from the at least one other sensor, said force prediction unit comprising a preprogrammed processor receiving the tire deformation input and the at least one other sensor input, said force prediction unit characterized by implementing preprogrammed equations having constants determined from previously collected data to determine from at least the tire deformation input and the at least one other sensor input an output corresponding to a predicted lateral force acting on a tire and outputting a predicted lateral force output corresponding to the predicted lateral force acting on the tire; and

(b) a control unit in circuit communication with said force prediction unit for receiving the predicted lateral force output and for being placed in circuit communication with vehicle actuators, said control unit characterized by altering the dynamic state of the vehicle via the actuators responsive at least in part to the predicted lateral force output from the force prediction unit.

39. The vehicle control system of claim 38, wherein said control unit has associated therewith a plurality of μ-slip curves, each of said μ-slip curves being associated with a different lateral force, said control unit implementing an anti-lock braking system based on a selected one of said μ-slip curves, and further wherein said control unit is characterized by selecting the of said plurality of μ-slip curves responsive at least in part to the predicted lateral force output from the force prediction unit and using the selected one of said plurality of μ-slip curves to implement anti-lock braking.

40. A vehicle control system comprising:

(a) a force prediction unit for being placed in circuit communication with a tire deformation sensor and at least one other sensor, receiving a tire deformation input from the tire deformation sensor, and receiving at least one other tire sensor input from the at least one other sensor, said force prediction unit comprising a preprogrammed processor receiving the tire deformation input and the at least one other sensor input, said force prediction unit characterized by implementing preprogrammed equations having constants determined from previously collected data to determine from at least the tire deformation input and the at least one other sensor input an output corresponding to a predicted vertical force acting on a tire and outputting a predicted vertical force output corresponding to the predicted vertical force acting on the tire; and

(b) a control unit in circuit communication with said force prediction unit for receiving the predicted vertical force output and for being placed in circuit communication with vehicle actuators, said control unit characterized by altering the dynamic state of the vehicle via the actuators responsive at least in part to the predicted vertical force output from the force prediction unit.

41. A method of predicting the circumferential torque or longitudinal force acting on a tire, comprising the steps of:

(a) providing a force prediction unit for being placed in circuit communication with a tire deformation sensor and at least one other sensor, receiving a tire deformation input from the tire deformation sensor, and receiving at least one other tire sensor input from the at least one other sensor, said force prediction unit comprising a preprogrammed processor receiving the tire deformation input and the at least one other sensor input, said force prediction unit characterized by implementing preprogrammed equations having

constants determined from previously collected data to determine from at least the tire deformation input and the at least one other sensor input an output corresponding to a predicted vertical force acting on a tire;

(b) collecting tire deformation input from the tire deformation sensor and the at least one other tire sensor input from the at least one other sensor; and

(c) determining with the force prediction unit the circumferential torque or longitudinal force acting on a tire from the collected tire deformation input and the collected at least one other tire sensor input.

42. A method of training a neural network to determine the circumferential torque or longitudinal force acting on a tire from a tire deformation sensor and at least one other sensor, comprising the steps of:

(a) collecting tire deformation input from a tire deformation sensor and at least one other tire sensor input from at least one other sensor;

(b) collecting an input corresponding to the circumferential torque or longitudinal force acting on the tire;

(c) training the neural network to predict the circumferential torque or longitudinal force acting on a tire using as training data at least the collected tire deformation input, the collected at least one other tire sensor input, and the collected input corresponding to the circumferential torque or longitudinal force acting on the tire.

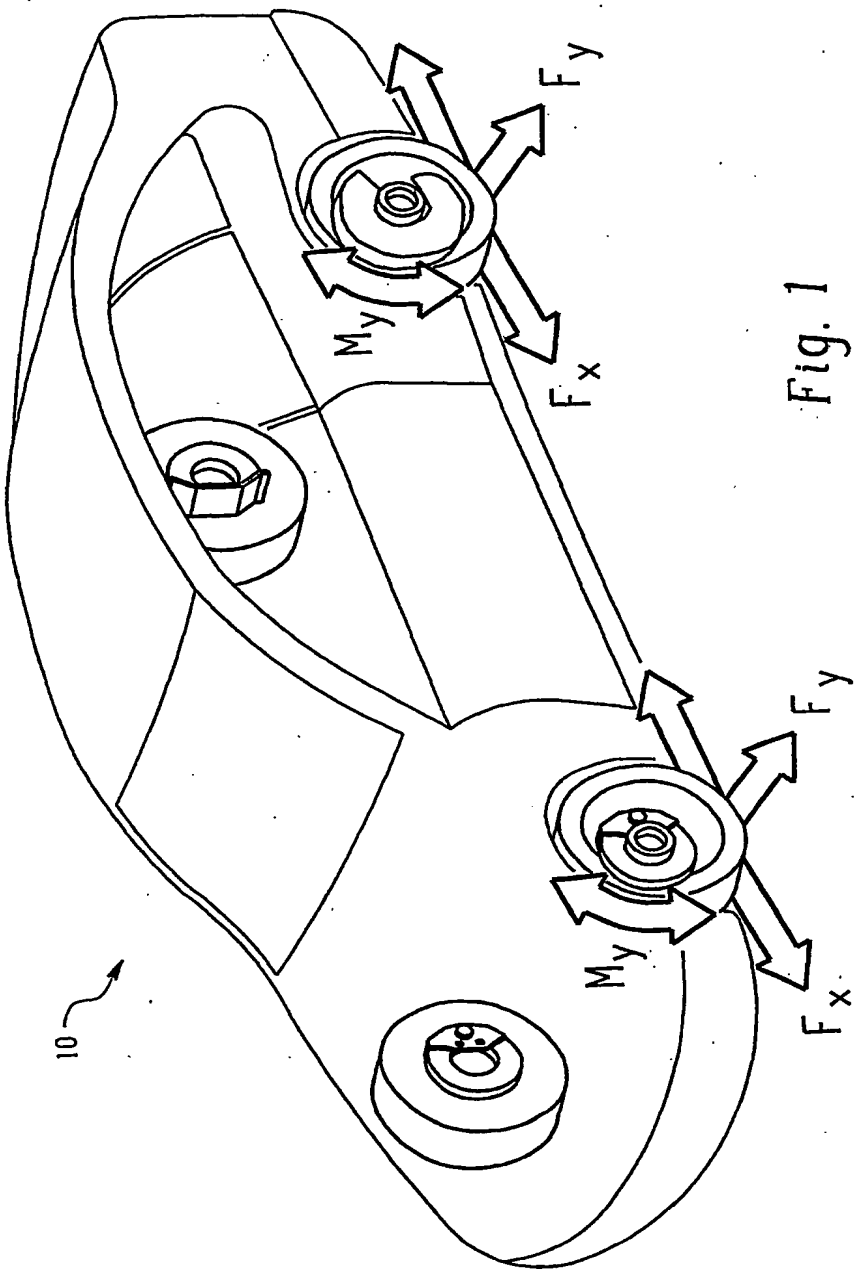

Fig. 1

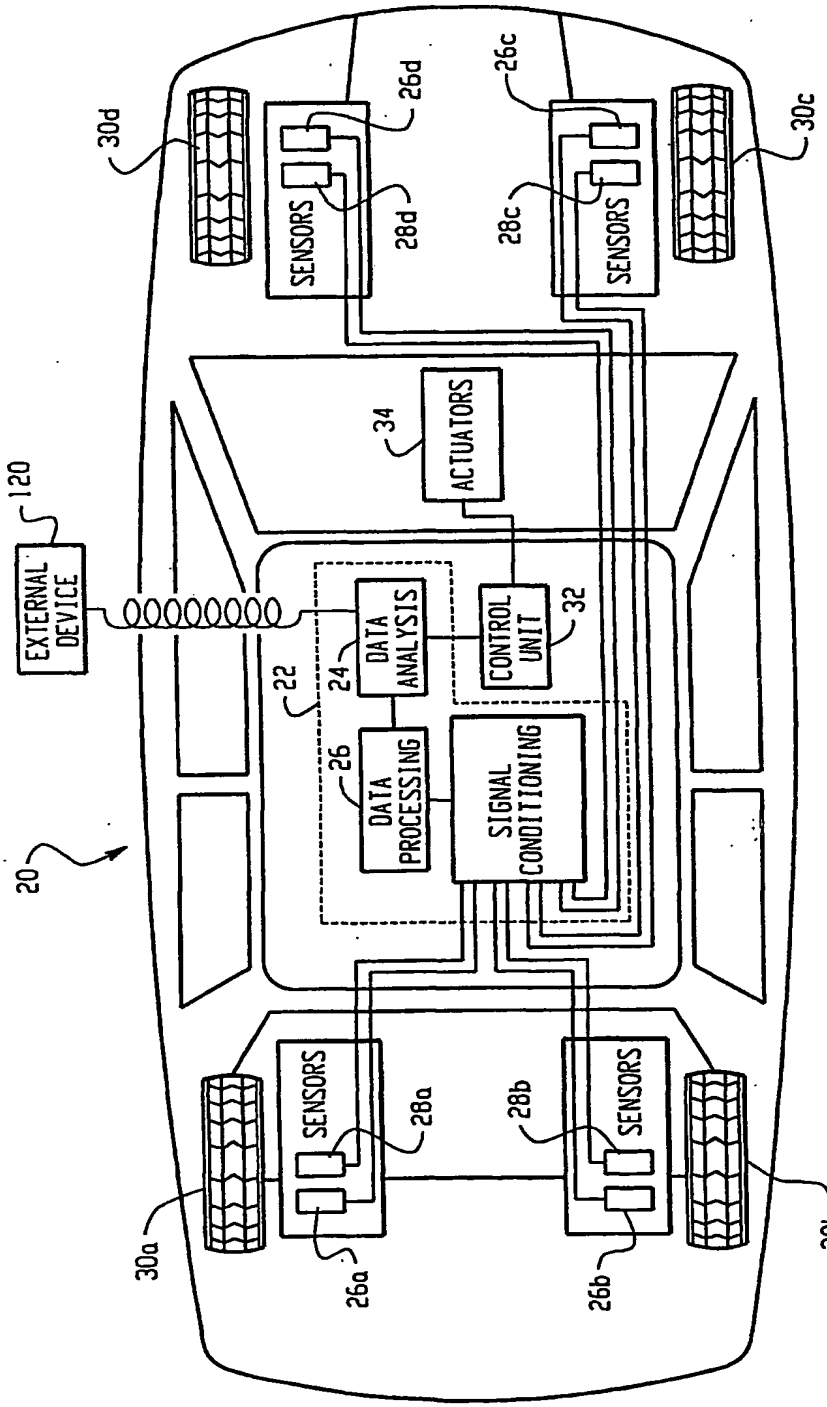
30d
26d
SENSORS
28d
26c
28c
SENSORS
30c
34
ACTUATORS
120
EXTERNAL DEVICE
22
24
DATA ANALYSIS
CONTROL UNIT
32
26
DATA PROCESSING
SIGNAL CONDITIONING
20
SENSORS
28a
28b
SENSORS
30a
26a
26b
30b

Fig. 2

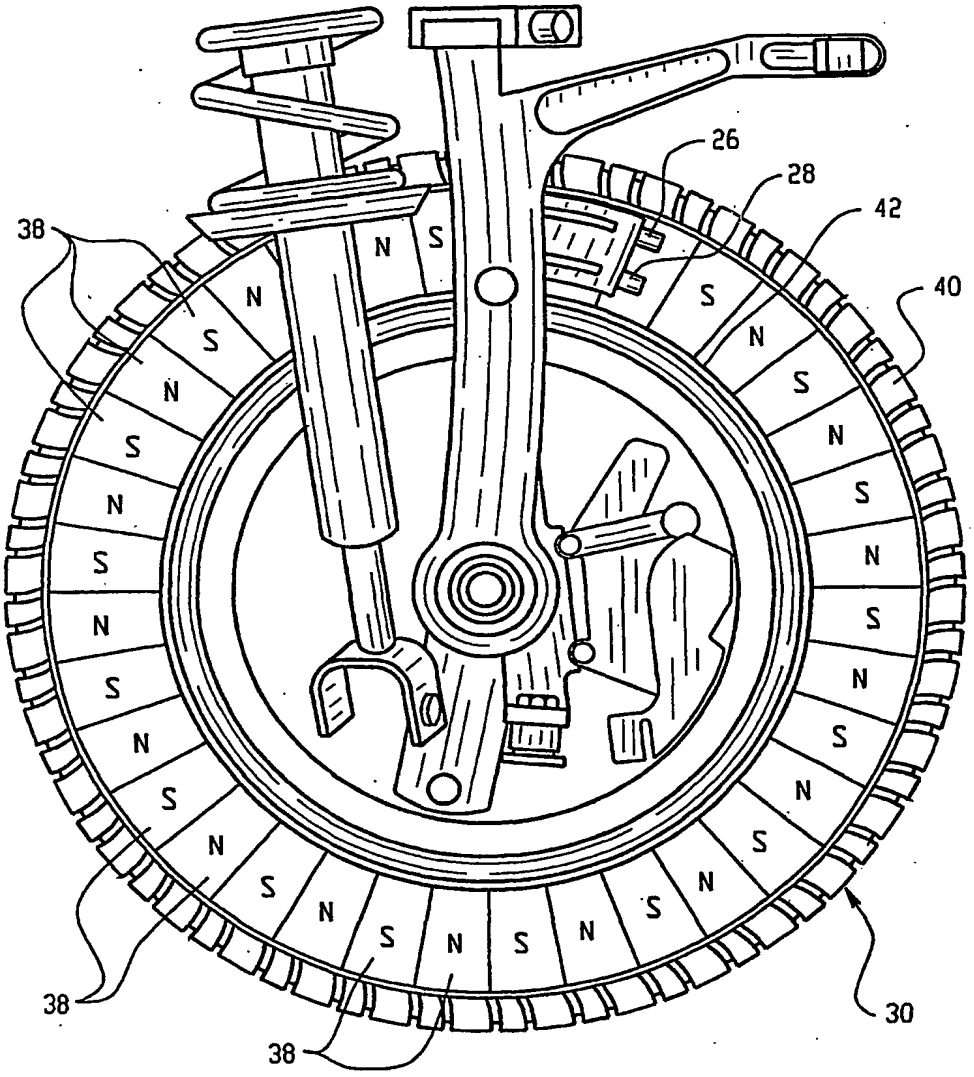

Fig. 3

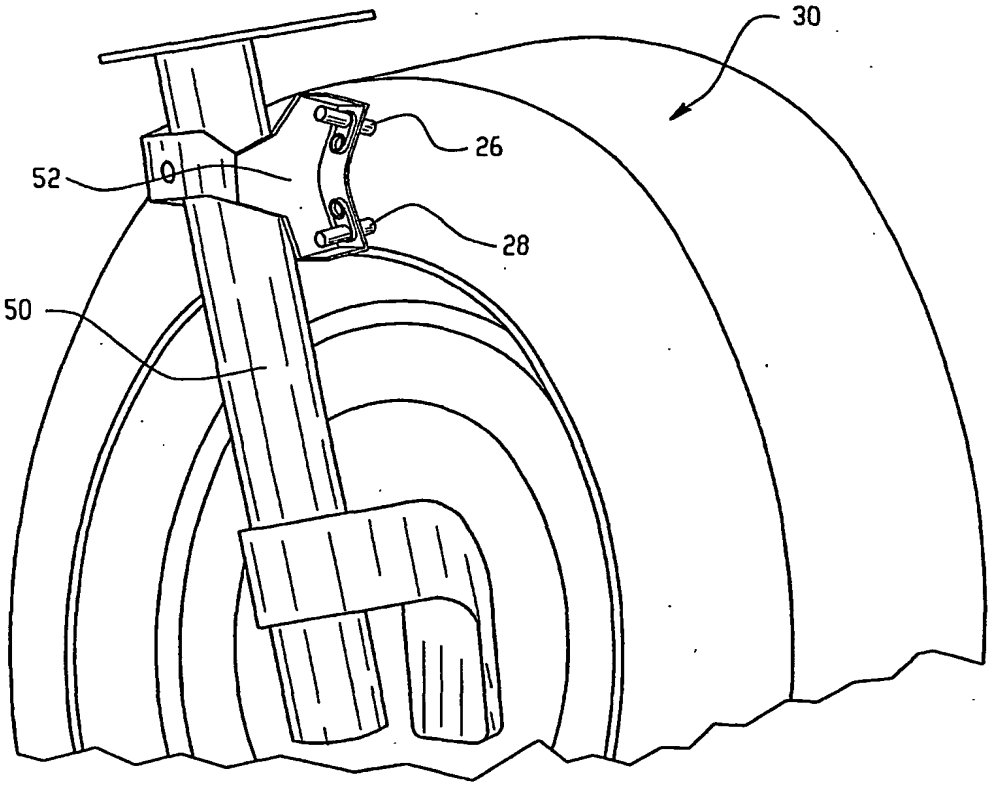

Fig. 4

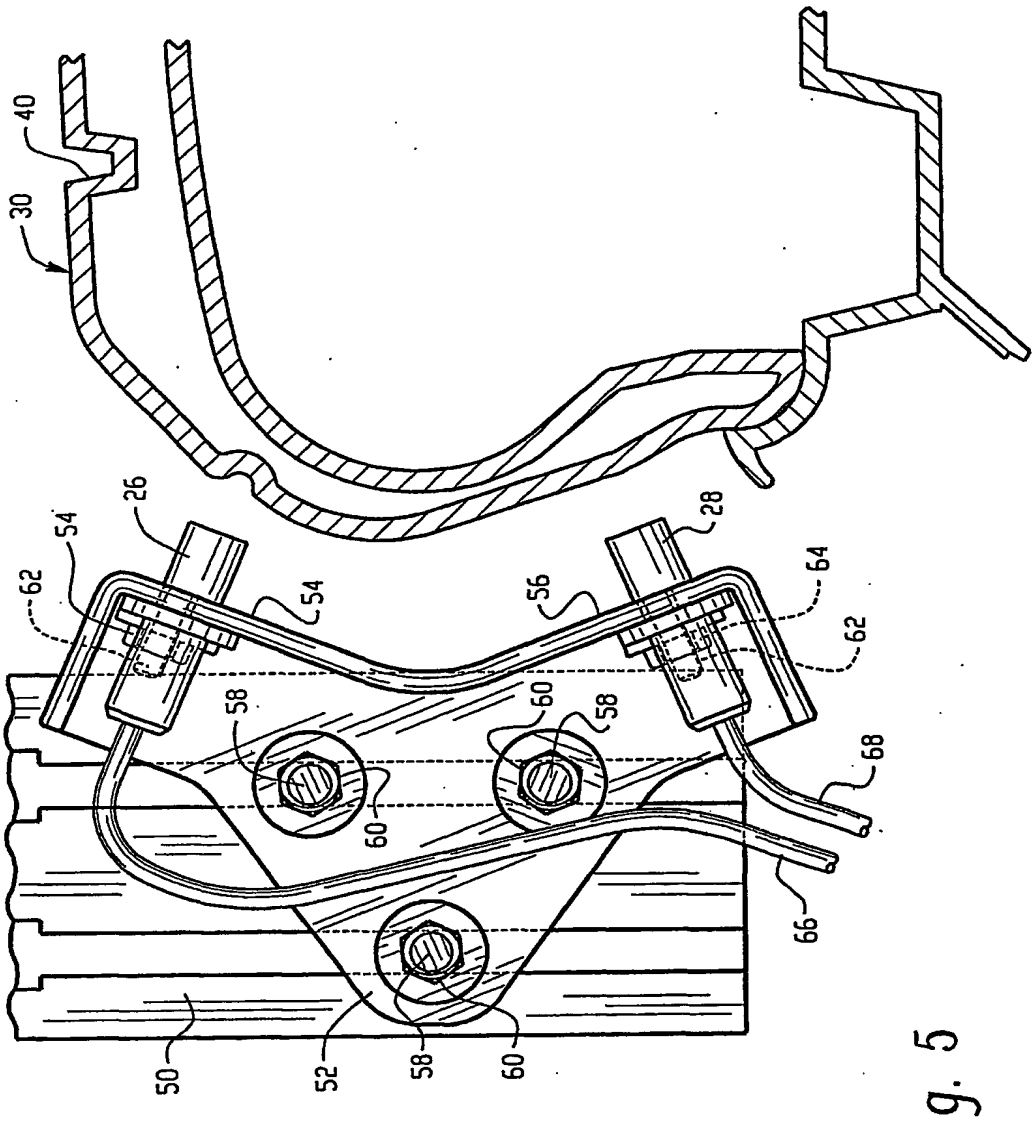

Fig. 5

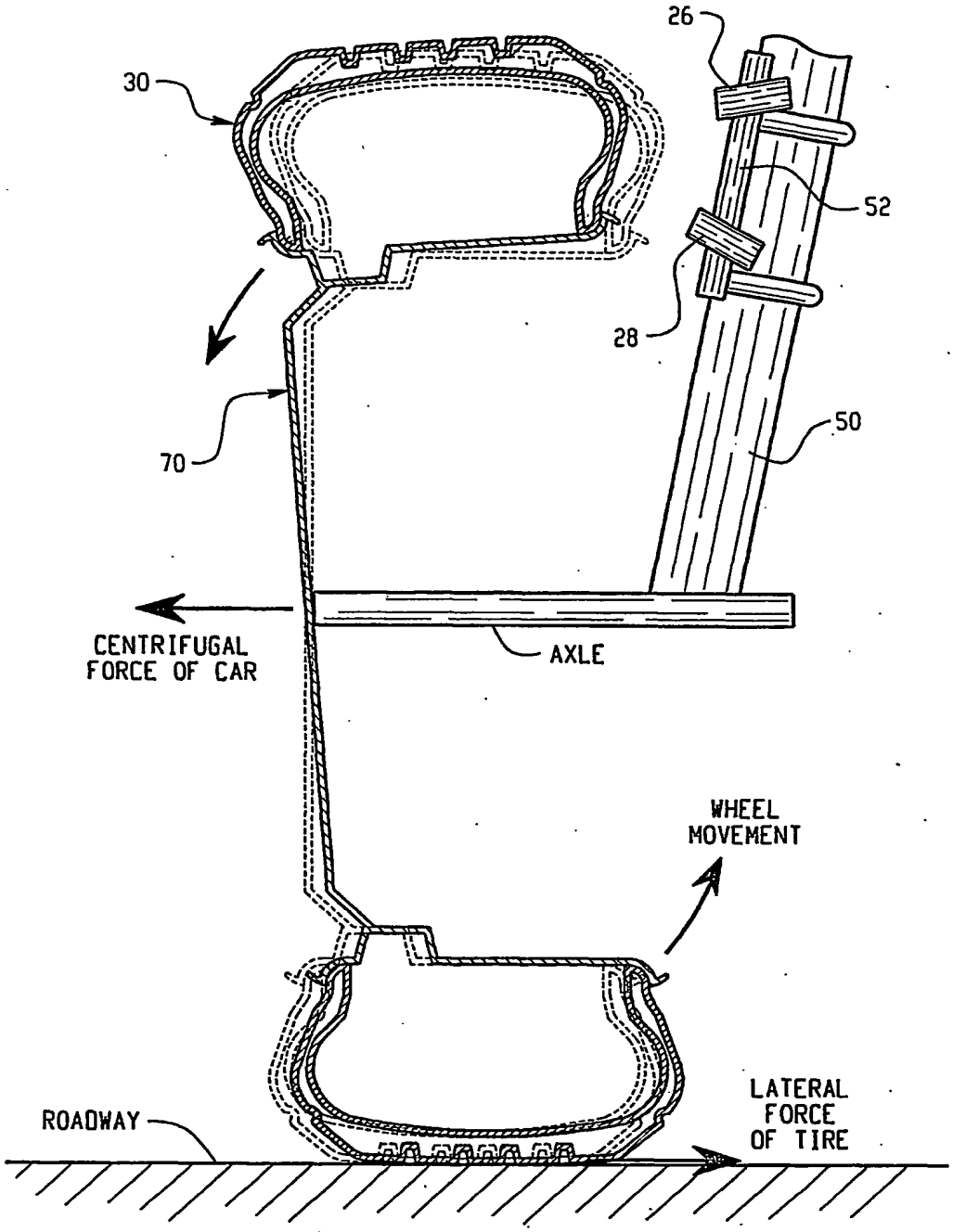
26
30
52
28
50
70
CENTRIFUGAL
FORCE OF CAR
AXLE
WHEEL
MOVEMENT
LATERAL
FORCE
OF TIRE
ROADWAY

Fig. 6

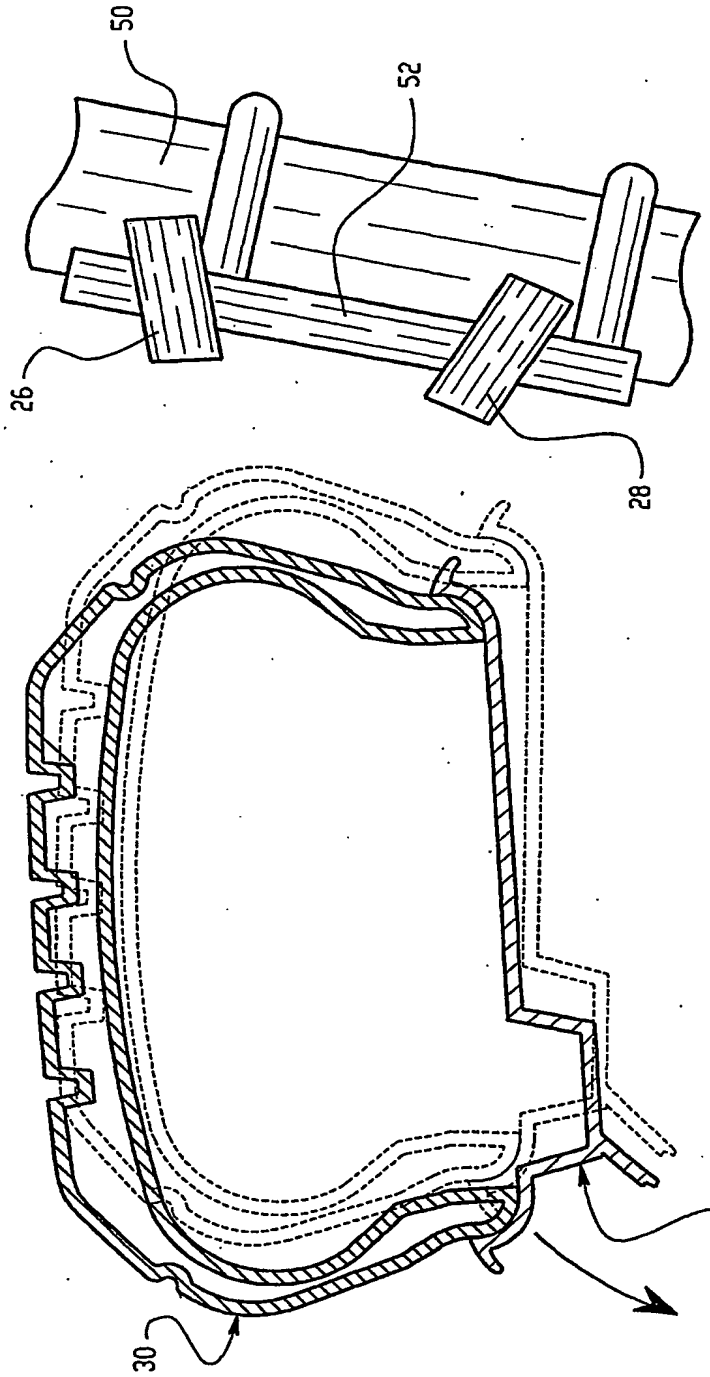

Fig. 7

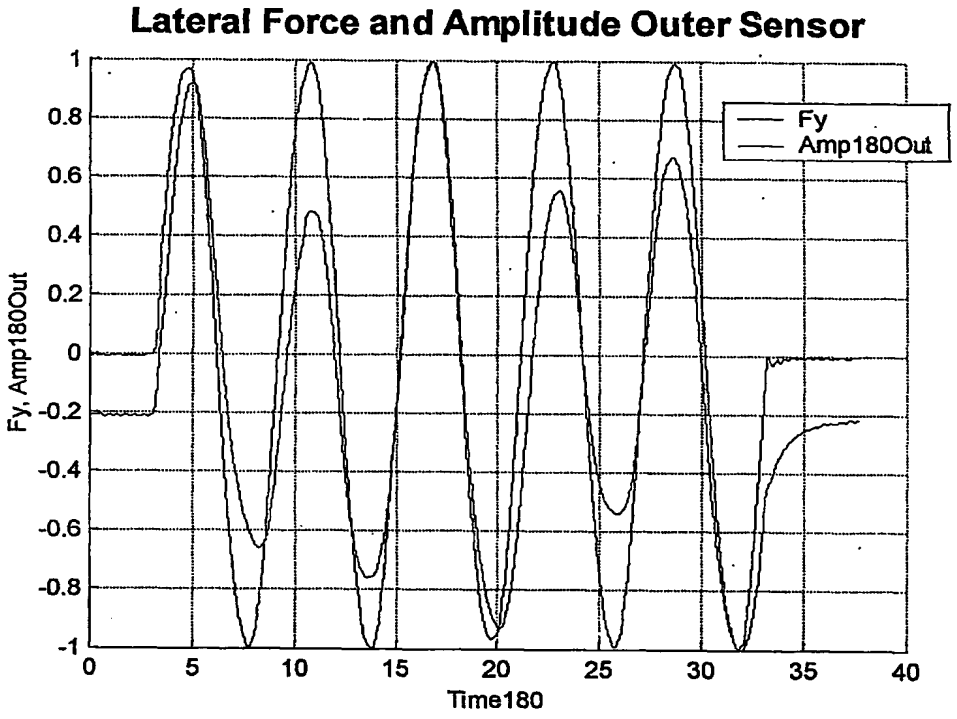
Lateral Force and Amplitude Outer Sensor
Fy
Amp180Out
Fy, Amp180Out
Time180
1
0.8
0.6
0.4
0.2
0
-0.2
-0.4
-0.6
-0.8
-1
0
5
10
15
20
25
30
35
40

Fig. 8

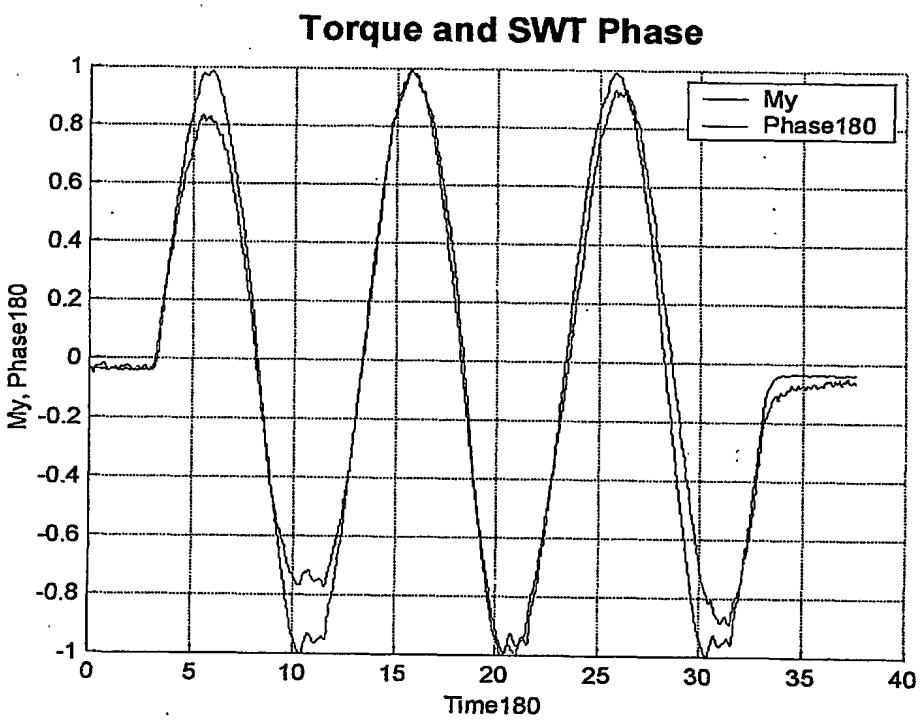
Torque and SWT Phase
My
Phase180
My, Phase180
Time180
1
0.8
0.6
0.4
0.2
0
-0.2
-0.4
-0.6
-0.8
-1
0
5
10
15
20
25
30
35
40

Fig. 9

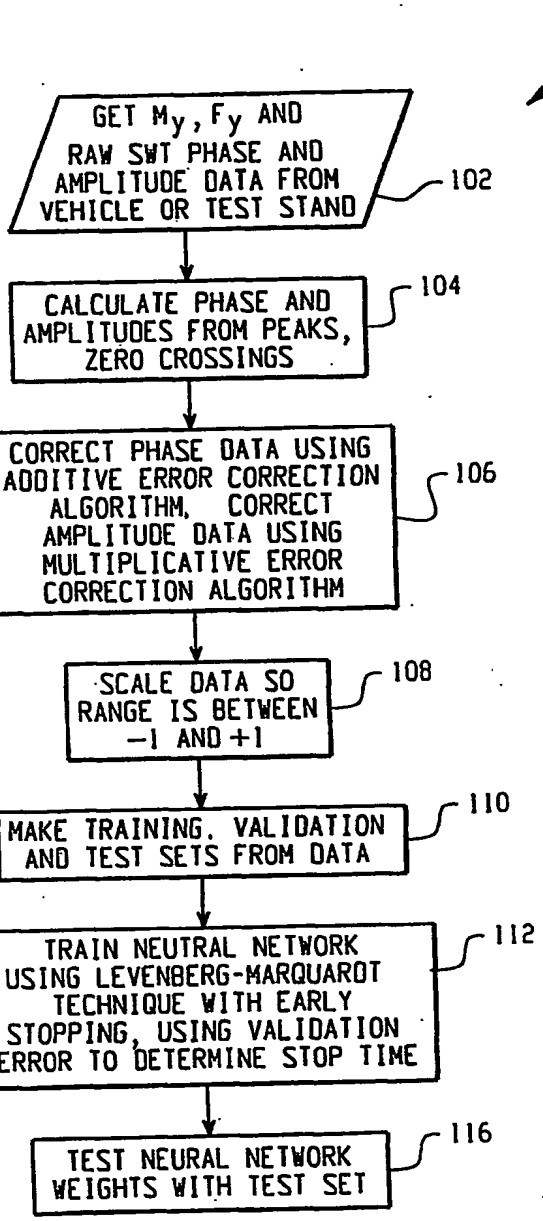
100
GET My, Fy AND RAW SWT PHASE AND AMPLITUDE DATA FROM VEHICLE OR TEST STAND
102
CALCULATE PHASE AND AMPLITUDES FROM PEAKS, ZERO CROSSINGS
104
CORRECT PHASE DATA USING ADDITIVE ERROR CORRECTION ALGORITHM, CORRECT AMPLITUDE DATA USING MULTIPLICATIVE ERROR CORRECTION ALGORITHM
106
SCALE DATA SO RANGE IS BETWEEN −1 AND +1
108
MAKE TRAINING, VALIDATION AND TEST SETS FROM DATA
110
TRAIN NEUTRAL NETWORK USING LEVENBERG-MARQUARDT TECHNIQUE WITH EARLY STOPPING, USING VALIDATION ERROR TO DETERMINE STOP TIME
112
TEST NEURAL NETWORK WEIGHTS WITH TEST SET
116

Fig. 10

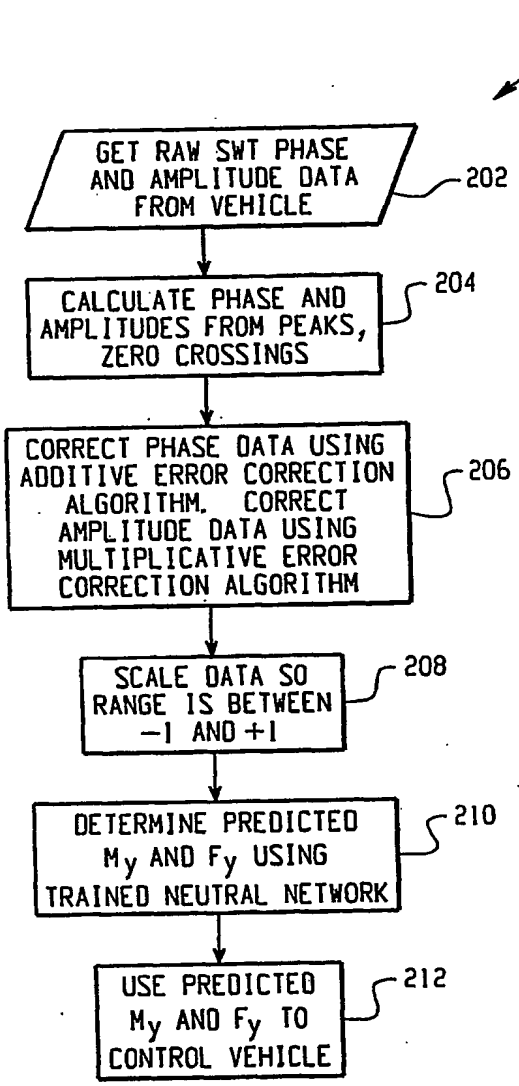
200
GET RAW SWT PHASE AND AMPLITUDE DATA FROM VEHICLE
202
CALCULATE PHASE AND AMPLITUDES FROM PEAKS, ZERO CROSSINGS
204
CORRECT PHASE DATA USING ADDITIVE ERROR CORRECTION ALGORITHM. CORRECT AMPLITUDE DATA USING MULTIPLICATIVE ERROR CORRECTION ALGORITHM
206
SCALE DATA SO RANGE IS BETWEEN −1 AND +1
208
DETERMINE PREDICTED My AND Fy USING TRAINED NEUTRAL NETWORK
210
USE PREDICTED My AND Fy TO CONTROL VEHICLE
212

Fig. 11

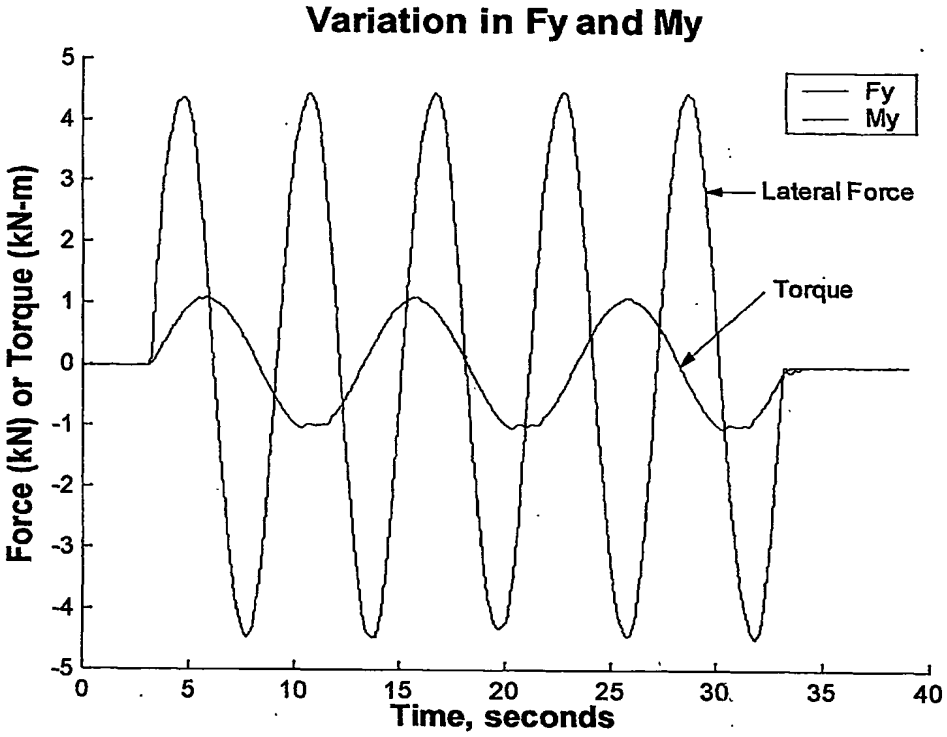
Variation in Fy and My
Force (kN) or Torque (kN-m)
Time, seconds
Fy
My
Lateral Force
Torque
5
4
3
2
1
0
-1
-2
-3
-4
-5
0
5
10
15
20
25
30
35
40

Fig. 12

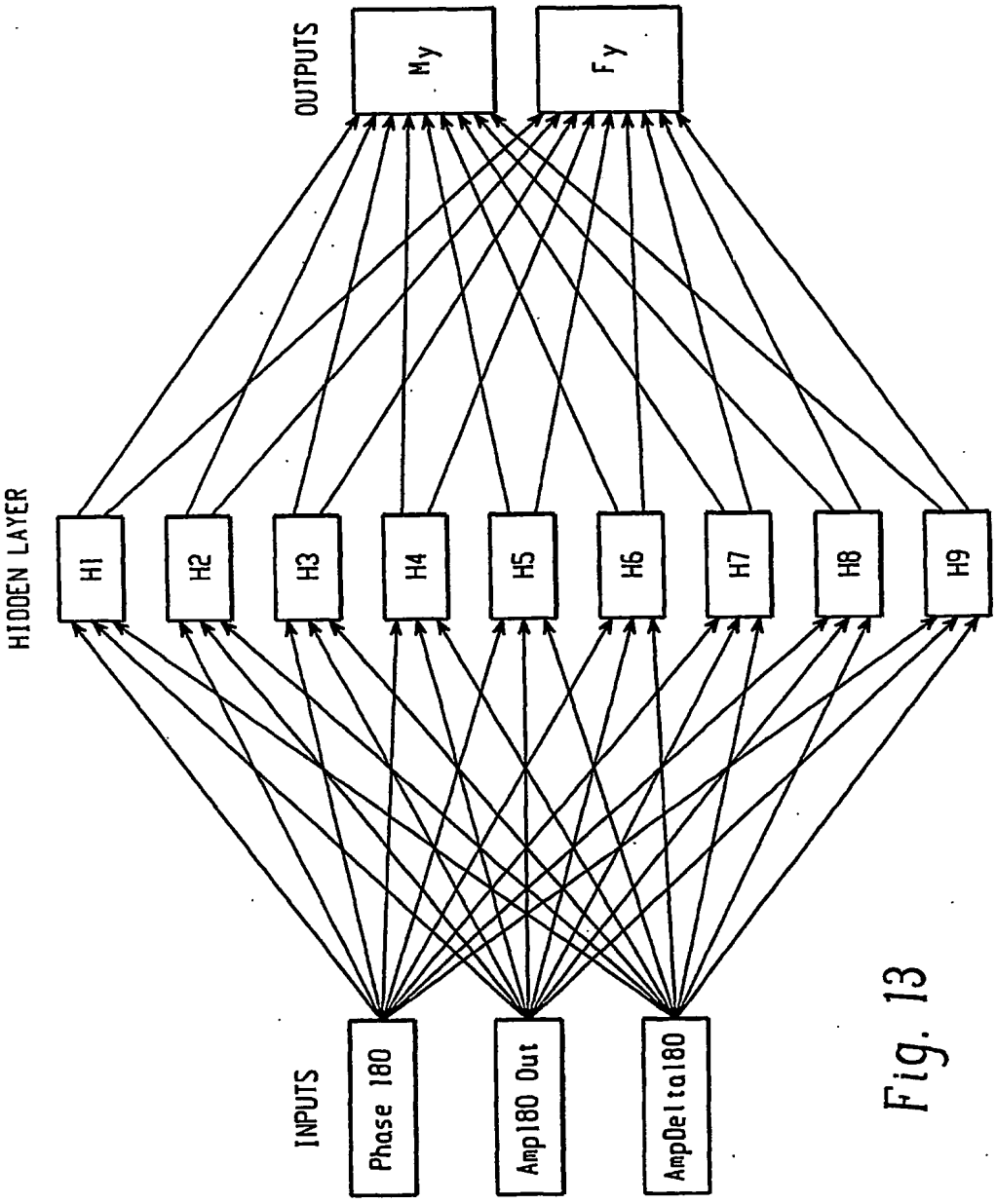
OUTPUTS
My
Fy
HIDDEN LAYER
H1
H2
H3
H4
H5
H6
H7
H8
H9
INPUTS
Phase 180
Amp180 Out
AmpDelta180

Fig. 13

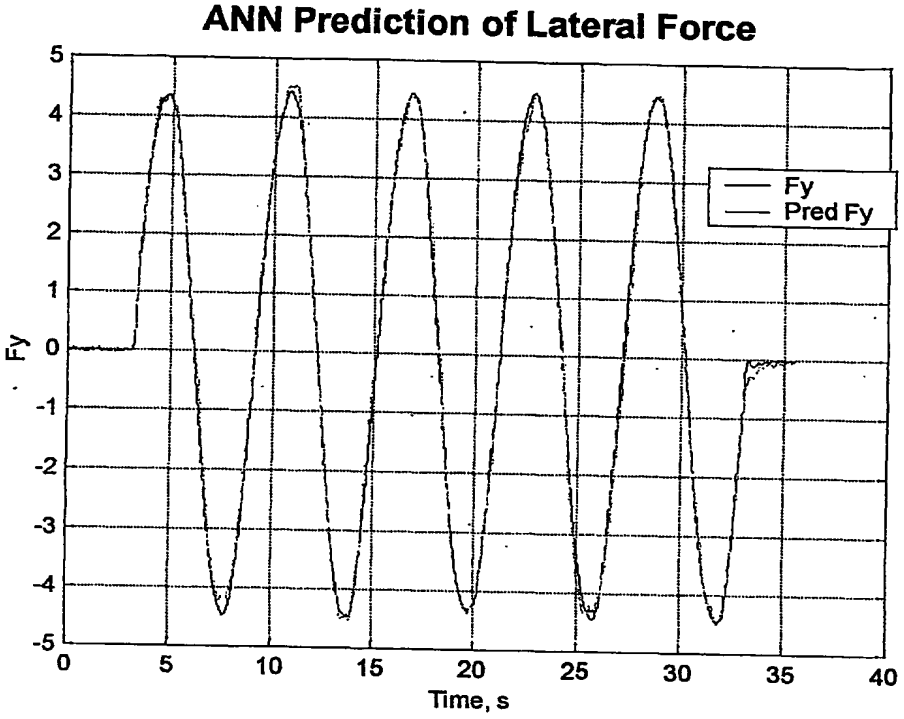
ANN Prediction of Lateral Force
Fy
Pred Fy
Fy
Time, s
5
4
3
2
1
0
-1
-2
-3
-4
-5
0
5
10
15
20
25
30
35
40

Fig. 14

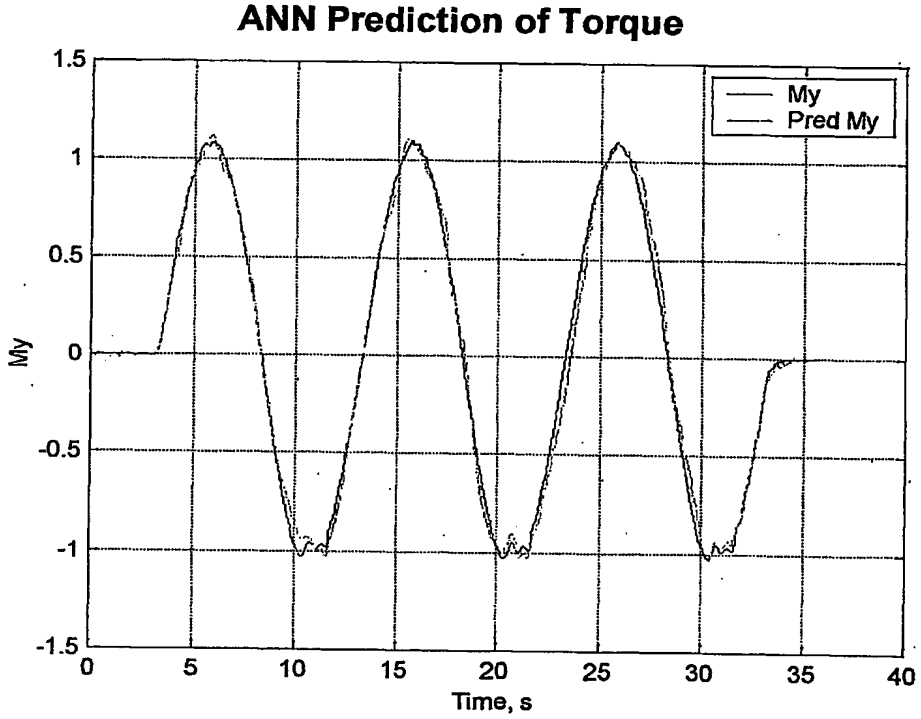
ANN Prediction of Torque
My
Pred My
My
Time, s
1.5
1
0.5
0
-0.5
-1
-1.5
0
5
10
15
20
25
30
35
40

Fig. 15

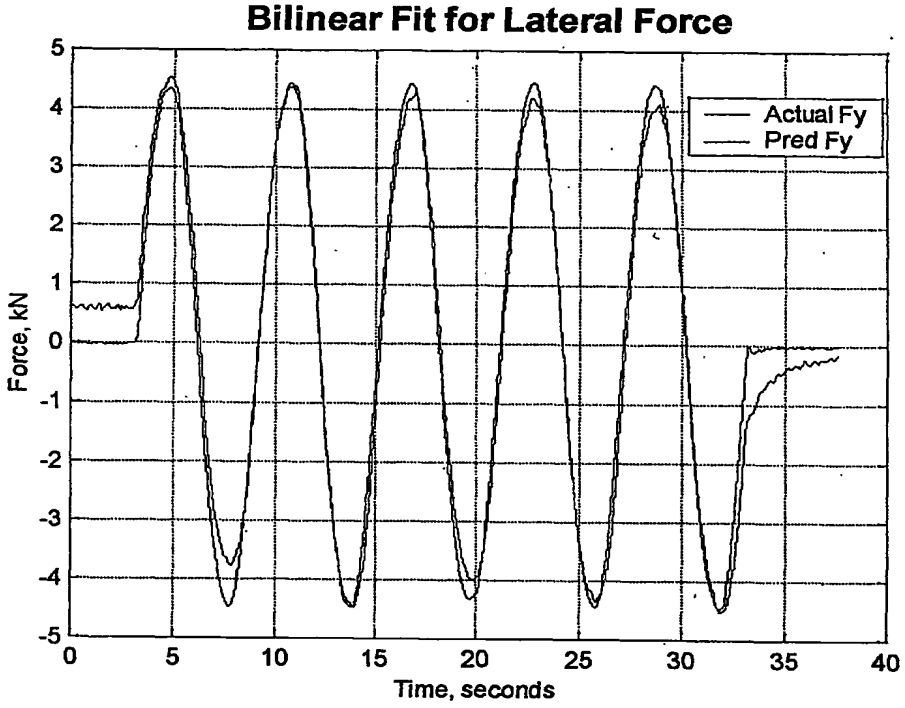
Bilinear Fit for Lateral Force
Actual Fy
Pred Fy
Force, kN
Time, seconds
5
4
3
2
1
0
-1
-2
-3
-4
-5
0
5
10
15
20
25
30
35
40

Fig. 16

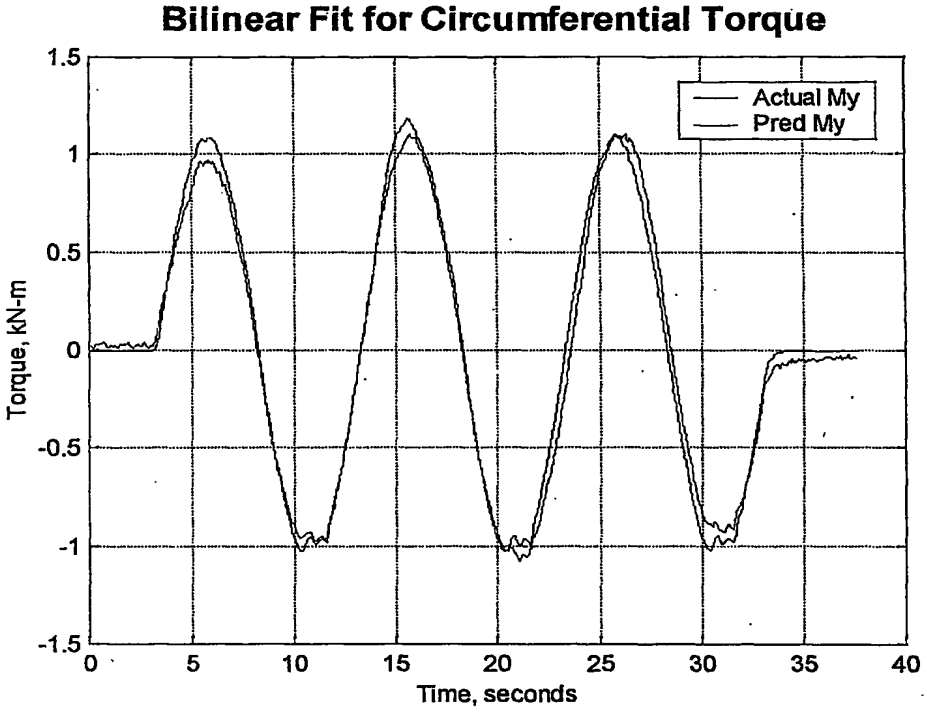
Bilinear Fit for Circumferential Torque
Actual My
Pred My
Torque, kN-m
Time, seconds
1.5
1
0.5
0
-0.5
-1
-1.5
0
5
10
15
20
25
30
35
40

Fig. 17

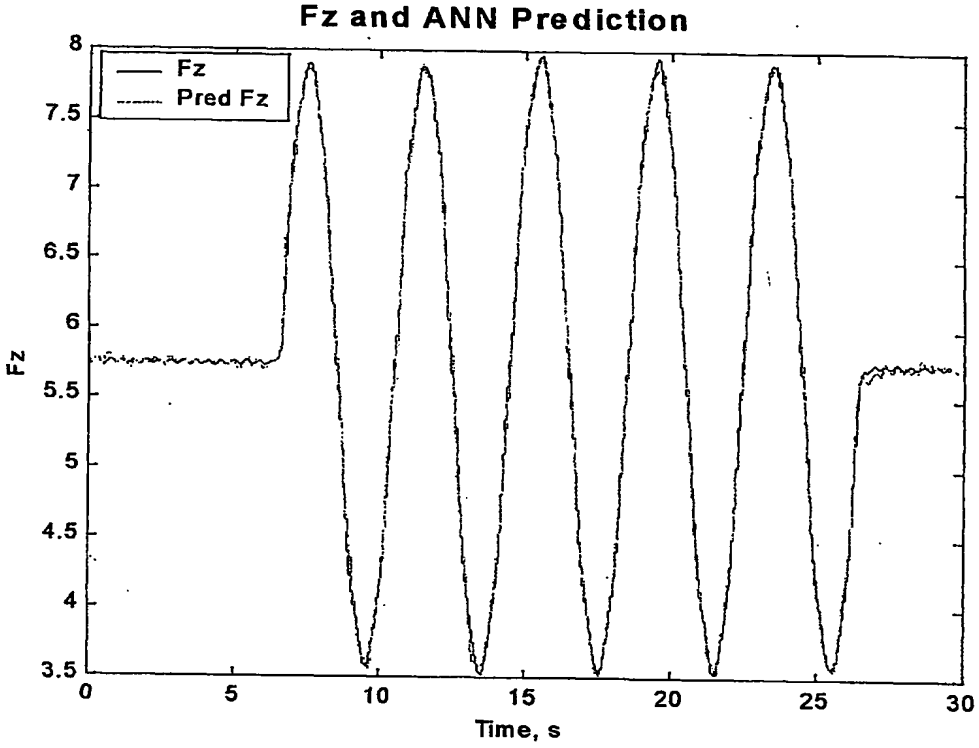
Fz and ANN Prediction
Fz
Pred Fz
Fz
Time, s
8
7.5
7
6.5
6
5.5
5
4.5
4
3.5
0
5
10
15
20
25
30

Fig. 18

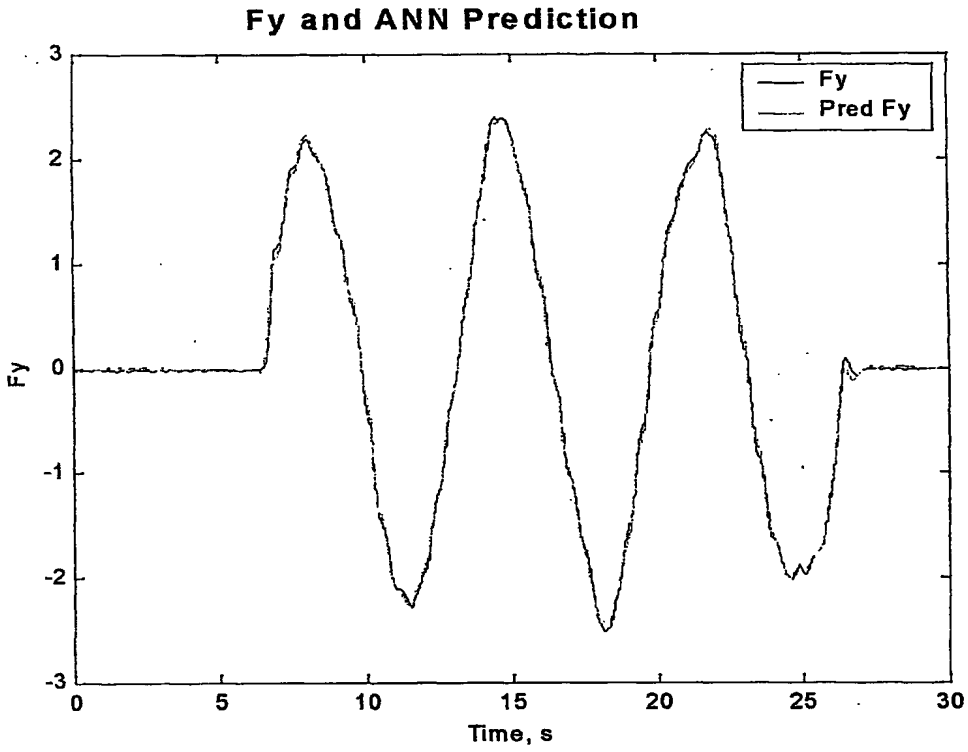
Fy and ANN Prediction
Fy
Pred Fy
Fy
Time, s
3
2
1
0
-1
-2
-3
0
5
10
15
20
25
30

Fig. 19

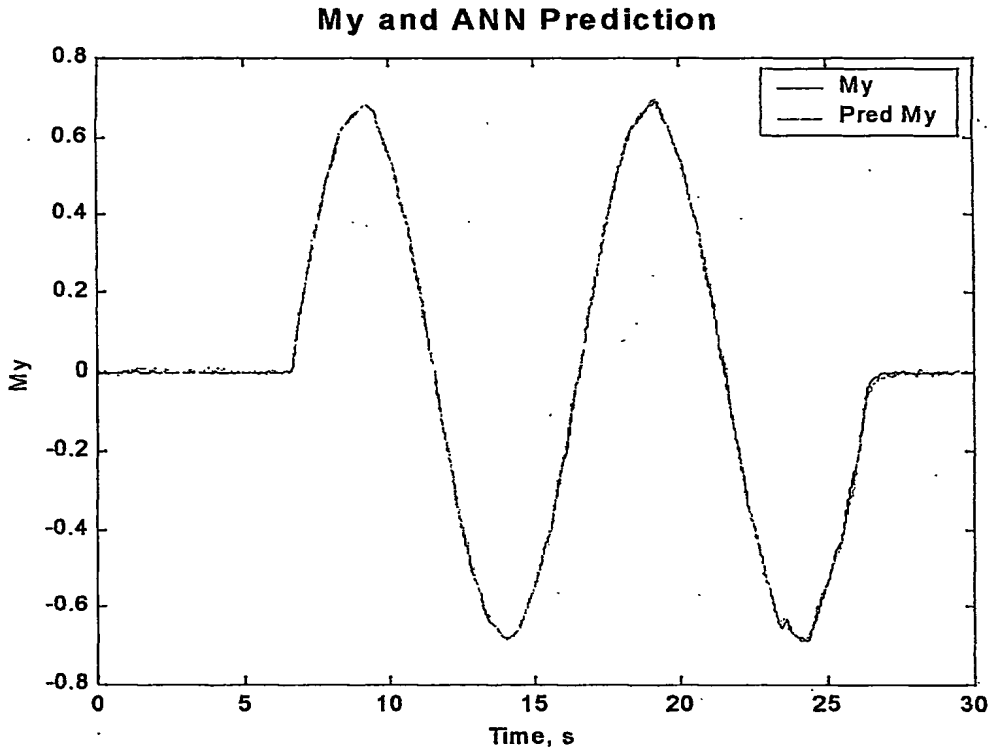
My and ANN Prediction
My
Pred My
My
Time, s
0.8
0.6
0.4
0.2
0
-0.2
-0.4
-0.6
-0.8
0
5
10
15
20
25
30

Fig. 20

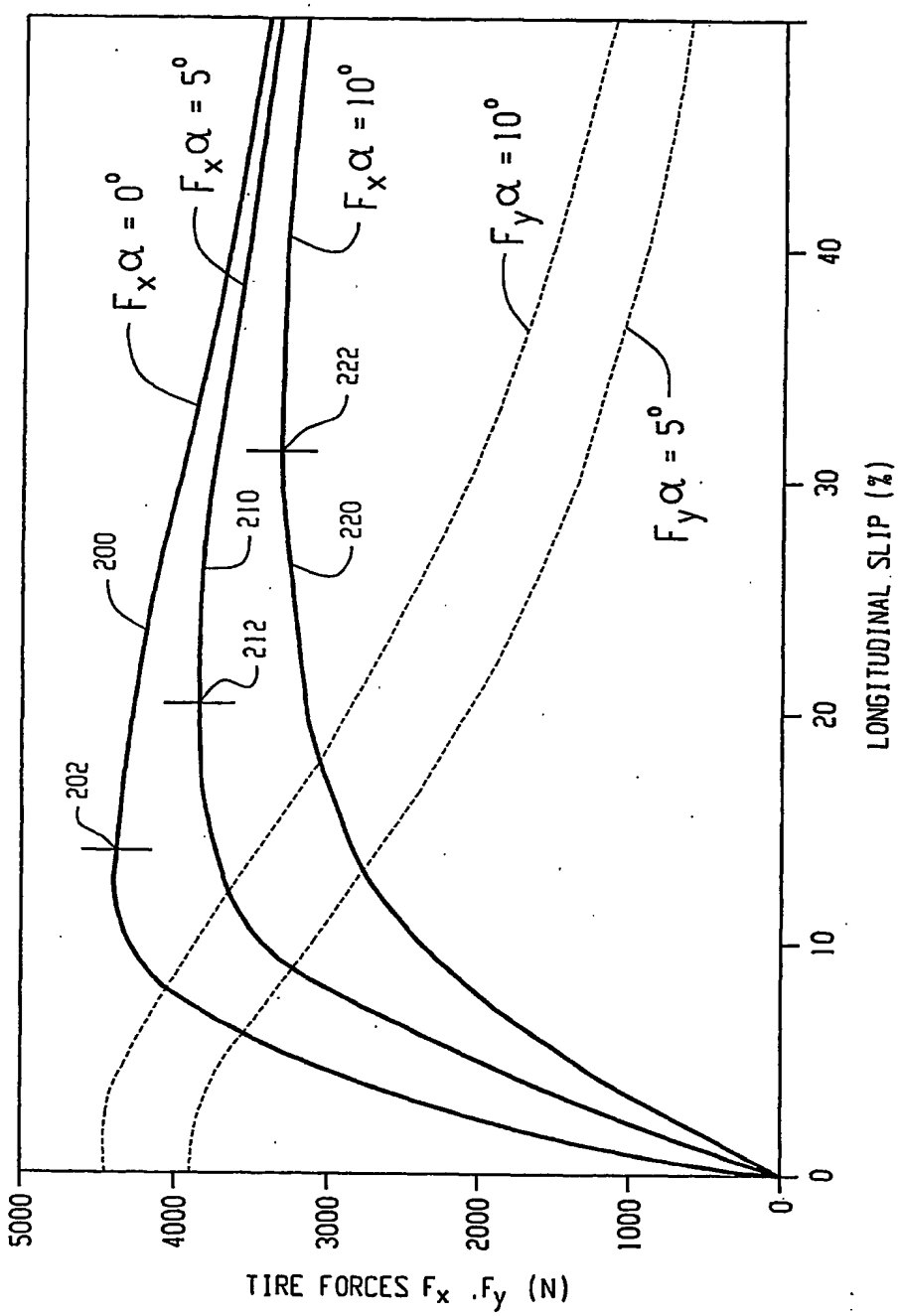
$F_x\alpha = 0°$
$F_x\alpha = 5°$
$F_x\alpha = 10°$
$F_y\alpha = 10°$
$F_y\alpha = 5°$
200
210
220
202
212
222
5000
4000
3000
2000
1000
0
TIRE FORCES F_x .F_y (N)
0
10
20
30
40
LONGITUDINAL SLIP (%)

Fig. 21

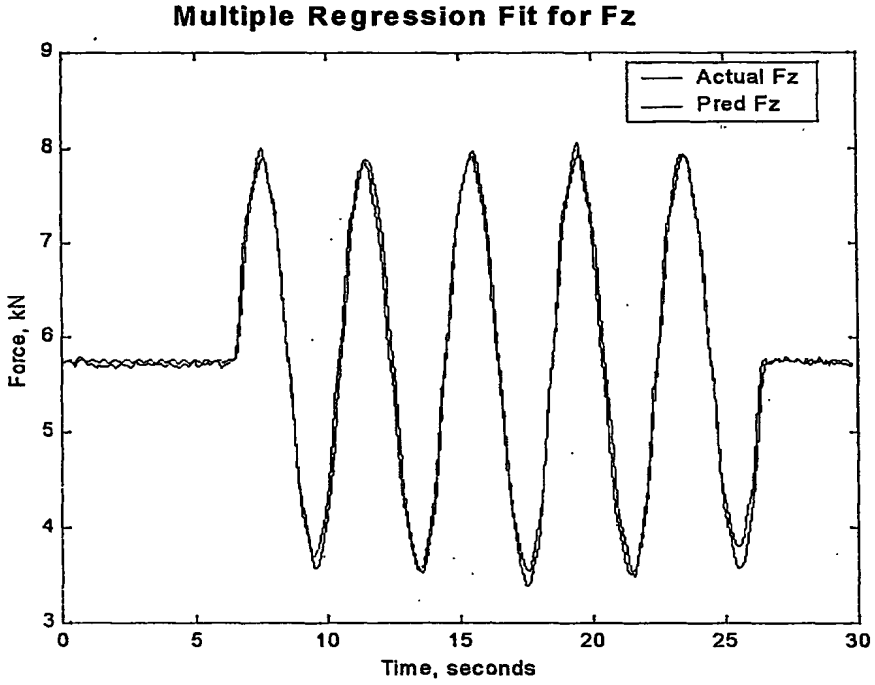
Multiple Regression Fit for Fz
Actual Fz
Pred Fz
Force, kN
Time, seconds
9
8
7
6
5
4
3
0
5
10
15
20
25
30

Fig. 22

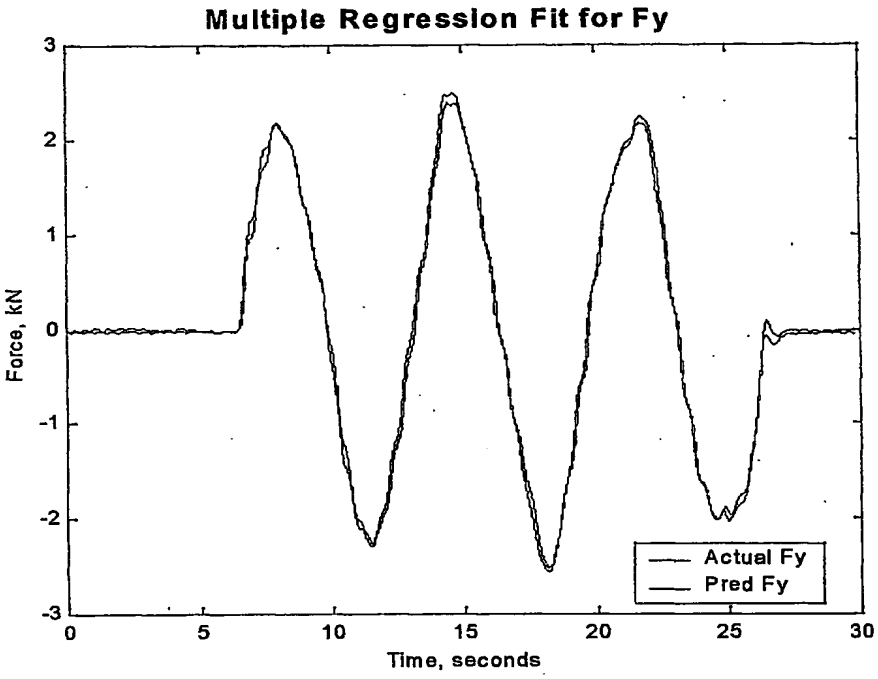
Multiple Regression Fit for Fy
Force, kN
Time, seconds
Actual Fy
Pred Fy
3
2
1
0
-1
-2
-3
0
5
10
15
20
25
30

Fig. 23

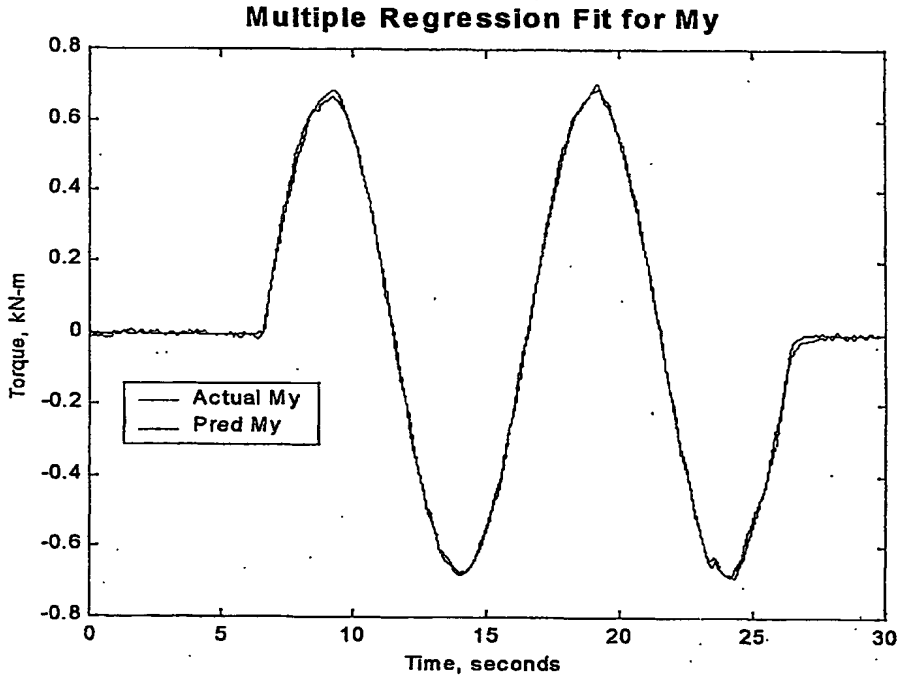
Multiple Regression Fit for My
Torque, kN-m
Time, seconds
Actual My
Pred My
0.8
0.6
0.4
0.2
0
-0.2
-0.4
-0.6
-0.8
0
5
10
15
20
25
30

Fig. 24

(12) INTERNATIONAL APPLICATION PUBLISHED UNDER THE PATENT COOPERATION TREATY (PCT)

(19) World Intellectual Property Organization
International Bureau

(43) International Publication Date
6 December 2001 (06.12.2001)

PCT

(10) International Publication Number
WO 01/92078 A3

(51) International Patent Classification[7]: B60T 8/00

(21) International Application Number: PCT/US01/17606

(22) International Filing Date: 31 May 2001 (31.05.2001)

(25) Filing Language: English

(26) Publication Language: English

(30) Priority Data:
09/584,230 31 May 2000 (31.05.2000) US

(71) Applicant *(for all designated States except US)*: CONTINENTAL AG [DE/DE]; Vahrenwalder Strasse 9, 30165 Hannover (DE).

(72) Inventor; and

(75) Inventor/Applicant *(for US only)*: GIUSTINO, James, M. [US/US]; 8801 Ferngrove Court, Waxhaw, NC 28173 (US).

(74) Agent: MOORHEAD, Sean, T.; Calfee, Halter & Griswold LLP, 1400 McDonald Investment Center, 800 Superior Avenue, Cleveland, OH 44114 (US).

(81) Designated States *(national)*: AE, AG, AL, AM, AT, AU, AZ, BA, BB, BG, BR, BY, BZ, CA, CH, CN, CO, CR, CU, CZ, DE, DK, DM, DZ, EC, EE, ES, FI, GB, GD, GE, GH, GM, HR, HU, ID, IL, IN, IS, JP, KE, KG, KP, KR, KZ, LC, LK, LR, LS, LT, LU, LV, MA, MD, MG, MK, MN, MW, MX, MZ, NO, NZ, PL, PT, RO, RU, SD, SE, SG, SI, SK, SL, TJ, TM, TR, TT, TZ, UA, UG, US, UZ, VN, YU, ZA, ZW.

(84) Designated States *(regional)*: ARIPO patent (GH, GM, KE, LS, MW, MZ, SD, SL, SZ, TZ, UG, ZW), Eurasian patent (AM, AZ, BY, KG, KZ, MD, RU, TJ, TM), European patent (AT, BE, CH, CY, DE, DK, ES, FI, FR, GB, GR, IE, IT, LU, MC, NL, PT, SE, TR), OAPI patent (BF, BJ, CF, CG, CI, CM, GA, GN, GW, ML, MR, NE, SN, TD, TG).

Published:
— *with international search report*

(88) Date of publication of the international search report:
4 April 2002

For two-letter codes and other abbreviations, refer to the "Guidance Notes on Codes and Abbreviations" appearing at the beginning of each regular issue of the PCT Gazette.

(54) Title: SYSTEM AND METHOD FOR PREDICTING TIRE FORCES USING TIRE DEFORMATION SENSORS

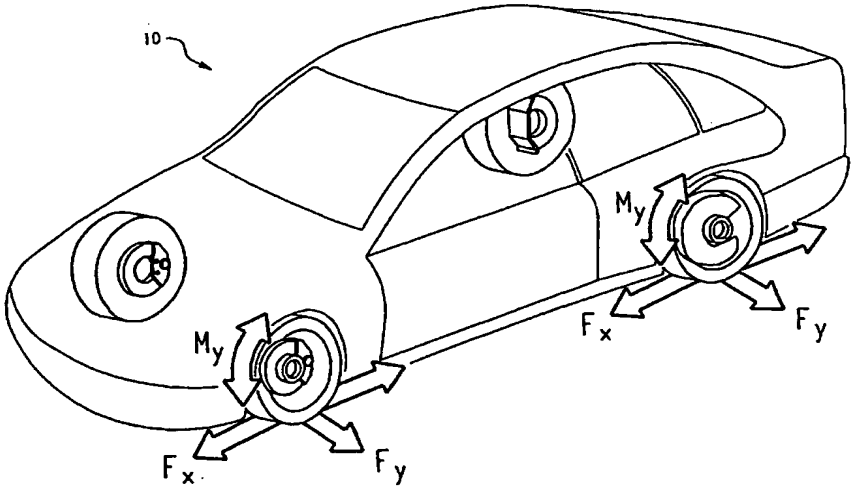

(57) Abstract: A system and method for predicting the forces generated in the tire contact patch from measurements of tire deformations, including separating the lateral force, the vertical force, and the circumferential torque using measurements of tire deformations. A system and method for using a trained neural network or bilinear equations to determine any combination or permutation of one or more of any of the following from tire sidewall deformation sensors, e.g., magnetic tire sidewall torsion measuring (SWT) sensors: the lateral force acting on the tire, the circumferential torque acting on the tire, the longitudinal force acting on the tire, the vertical force acting on the tire, and forces and/or torques having any one or more of the foregoing as components thereof.

WO 01/92078 A3

INTERNATIONAL SEARCH REPORT

Inter ·lonal Application No
PC1/US 01/17606

A. CLASSIFICATION OF SUBJECT MATTER
IPC 7 B60T8/00

According to International Patent Classification (IPC) or to both national classification and IPC

B. FIELDS SEARCHED

Minimum documentation searched (classification system followed by classification symbols)
IPC 7 B60T B60C

Documentation searched other than minimum documentation to the extent that such documents are included in the fields searched

Electronic data base consulted during the international search (name of data base and, where practical, search terms used)
EPO-Internal, WPI Data, PAJ, COMPENDEX

C. DOCUMENTS CONSIDERED TO BE RELEVANT

Category *	Citation of document, with indication, where appropriate, of the relevant passages	Relevant to claim No.
X	US 5 913 240 A (BECHERER THOMAS ET AL) 15 June 1999 (1999-06-15)	1,10
A	column 16, line 6 - line 11 claims 38-41,43-45 figure 1	11,20, 21,30, 37,38,40
A	US 5 864 056 A (BELL LARRY D ET AL) 26 January 1999 (1999-01-26) figure 8	1,11,37, 38

-/--

[X] Further documents are listed in the continuation of box C.

[X] Patent family members are listed in annex.

* Special categories of cited documents :

"A" document defining the general state of the art which is not considered to be of particular relevance

"E" earlier document but published on or after the international filing date

"L" document which may throw doubts on priority claim(s) or which is cited to establish the publication date of another citation or other special reason (as specified)

"O" document referring to an oral disclosure, use, exhibition or other means

"P" document published prior to the international filing date but later than the priority date claimed

"T" later document published after the international filing date or priority date and not in conflict with the application but cited to understand the principle or theory underlying the invention

"X" document of particular relevance; the claimed invention cannot be considered novel or cannot be considered to involve an inventive step when the document is taken alone

"Y" document of particular relevance; the claimed invention cannot be considered to involve an inventive step when the document is combined with one or more other such documents, such combination being obvious to a person skilled in the art.

"&" document member of the same patent family

Date of the actual completion of the international search	Date of mailing of the international search report
19 December 2001	16/01/2002

Name and mailing address of the ISA	Authorized officer
European Patent Office, P.B. 5818 Patentlaan 2 NL - 2280 HV Rijswijk Tel. (+31-70) 340-2040, Tx. 31 651 epo nl, Fax: (+31-70) 340-3016	Colonna, M

1

Form PCT/ISA/210 (second sheet) (July 1992)

INTERNATIONAL SEARCH REPORT

Inter ional Application No
PCT/US 01/17606

C.(Continuation) DOCUMENTS CONSIDERED TO BE RELEVANT

Category °	Citation of document, with indication, where appropriate, of the relevant passages	Relevant to claim No.
A	PALKOVICS L ET AL: "Neural network representation of tyre characteristics: the neuro-tyre" INT J VEH DES:INTERNATIONAL JOURNAL OF VEHICLE DESIGN 1993 PUBL BY INDERSCIENCE ENTERPRISES LTD, GENEVA AEROPORT 15, SWITZ, vol. 14, no. 5-6, 1993, pages 563-591, XP002186057 Abstract	1,2,11, 12,21, 22,42

1

Form PCT/ISA/210 (continuation of second sheet) (July 1992)

INTERNATIONAL SEARCH REPORT

Information on patent family members

International Application No
PCT/US 01/17606

Patent document cited in search report	Publication date	Patent family member(s)	Publication date
US 5913240 A	15-06-1999	DE 4435160 A1	04-04-1996
		AU 3653295 A	26-04-1996
		BR 9509168 A	30-09-1997
		CA 2212219 A1	11-04-1996
		DE 19581107 D2	12-02-1998
		DE 59504584 D1	28-01-1999
		WO 9610505 A1	11-04-1996
		EP 0783419 A1	16-07-1997
		ES 2129857 T3	16-06-1999
		JP 10506346 T	23-06-1998
		US 6161431 A	19-12-2000
US 5864056 A	26-01-1999	NONE	